A stable fixed point method for the numerical simulation of a kinetic collisional sheath

Mehdi Badsi, Christophe Berthon, Anaïs Crestetto

A stable fixed point method for the numerical simulation of a kinetic collisional sheath

Mehdi Badsi*, Christophe Berthon, Anaïs Crestetto

Université de Nantes, CNRS UMR 6629, Laboratoire de Mathématiques Jean Leray, 2 rue de la Houssinière, BP 92208, 44322 Nantes, France

Abstract

This work introduces a numerical fixed point method to approximate the solutions of a Vlasov-Poisson-Boltzmann boundary value problem which arises when modeling a bi-species collisional sheath. Our method relies on the exact integration of the transport equations by means of the characteristic curves. A special care is given about the choice of a suitable phase space discretization together with the use of adequate quadrature formulas so as to ensure that the numerical fixed point method is stable. Numerical experiments are carried out in order to illustrate the effects of the various physical parameters that are in the scope of the analysis. Some results going beyond the scope of the analysis are also given.

Keywords: stationary transport problems, Vlasov-Poisson-Boltzmann boundary value problem, collisional sheaths, fixed point method, characteristic curves

1. Introduction

Plasma interacting with material boundaries are ubiquitous in applications. A well-known physical feature of a plasma interacting with an isolated partially absorbing surface, is the development near the surface of a thin positively charged boundary layer called the Debye sheath. The Debye sheath can be mathematically described by a steady state regime where the flows of ions and electrons reaching the wall are equal [23, 8, 27]. The mathematical and physical foundations of plasma sheaths in the case where particles do not collide are now well-established [4, 2, 15, 14]. When particles suffer from

*Corresponding author

Email address: `mehdi.badsi@univ-nantes.fr` (Mehdi Badsi)

Preprint submitted to Elsevier *November 3, 2020*

collisions several models have been proposed in the literature [26, 24, 20]. In this work we are interested in the numerical approximation of the bi-species Vlasov-Poisson-Boltzmann model studied in [3]. The model reads as follows:

$$\begin{cases} v\partial_x f_i - \partial_x\phi\partial_v f_i = -\nu Q(f_i), & (x,v) \in (0,1)\times\mathbb{R}, \quad (1)\\ v\partial_x f_e + \dfrac{1}{\mu}\partial_x\phi\partial_v f_e = 0, & (x,v)\in(0,1)\times\mathbb{R}, \quad (2)\\ -\varepsilon^2\partial_{xx}\phi = n_i(x) - n_e(x), & x\in(0,1), \quad (3)\end{cases}$$

where the unknowns are the ions and electrons densities in the phase space $f_i : (x,v) \in [0,1]\times\mathbb{R} \mapsto f_i(x,v) \in \mathbb{R}^+$, $f_e : (x,v) \in [0,1]\times\mathbb{R} \mapsto f_e(x,v) \in \mathbb{R}^+$, and the electrostatic potential $\phi : x \in [0,1] \mapsto \phi(x) \in \mathbb{R}$. In this model, $\nu > 0$ is a normalized collision frequency between ions and a cold neutral gas, $\mu > 0$ denotes the mass ratio between electrons and ions, $\varepsilon > 0$ is a normalized Debye length, $Q(f_i)$ is a collision operator which takes the form of a linear relaxation operator towards a mono-kinetic distribution (see [1, 28, 6, 24] for more details):

$$\forall (x,v)\in(0,1)\times\mathbb{R}, \quad Q(f_i)(x,v) := f_i(x,v) - \left(\int_{\mathbb{R}} f_i(x,v)dv\right)\delta_{v=0}, \quad (4)$$

where $\delta_{v=0}$ is the Dirac measure supported at the point $v = 0$. The macroscopic densities are defined by :

$$\forall x \in [0,1] \quad n_i(x) := \int_{\mathbb{R}} f_i(x,v)dv, \quad n_e(x) := \int_{\mathbb{R}} f_e(x,v)dv. \quad (5)$$

The system (1)-(3) is supplemented with the following boundary conditions:

$$\begin{cases} f_i(0,v>0) = f_i^{\mathrm{inc}}(v), & f_i(1,v<0) = 0, \quad (6)\\ f_e(0,v>0) = n_0 f_e^{\mathrm{inc}}(v), & f_e(1,v<0) = \alpha f_e(1,-v), \quad (7)\\ \phi(0) = 0, & \phi(1) = \phi_{\mathrm{wall}}, \quad (8)\end{cases}$$

where $f_i^{\mathrm{inc}} : (0,+\infty) \to \mathbb{R}^+$, $f_e^{\mathrm{inc}} : (0,+\infty) \to \mathbb{R}^+$ stand for incoming particles densities that model the flows of particles that come from the plasma ($x = 0$). Since electrons are usually well described by Maxwellian distributions in the core plasma (see [27] for a physical justification), the incoming electrons density to be considered here is a normalized semi-Maxwellian

$$f_e^{\mathrm{inc}}(v) = \sqrt{\frac{2\mu}{\pi}}e^{-\frac{\mu v^2}{2}}, \quad \forall v > 0. \quad (9)$$

At the wall ($x = 1$), ions particles are absorbed while for the electrons a fraction $\alpha \in [0,1]$ of the particles is re-emitted from the wall specularly. The pair $(n_0, \phi_{\text{wall}}) \in (0, +\infty) \times (-\infty, 0)$ plays the role of an unknown which has to be determined in such a way that the solutions f_i, f_e, ϕ to (1)-(8) satisfy the additional equations

$$\begin{cases} n_i(0) = n_e(0), & (10) \\ J_i = J_e & (11) \end{cases}$$

where the current densities are defined by

$$\forall x \in [0,1] \quad J_i := \int_{\mathbb{R}} f_i(x,v) v dv, \quad J_e := \int_{\mathbb{R}} f_e(x,v) v dv. \tag{12}$$

Note that an integration in velocity of the equations (1)-(2) yields that the current densities are constant in space. The existence of weak solutions for the system (1)-(12) has been proven in [3]. We refer to Theorem 3.1 of the aforementioned reference for a precise statement of the existence result. To briefly summarize the result, it is shown that there is a critical re-emission coefficient $\alpha_c \approx 1$ such that for any $0 \leq \alpha \leq \alpha_c < 1$ and for any incoming ions density f_i^{inc} that belongs to a standard class of regularity and additionally satisfies

- the admissibility condition

$$\frac{\int_0^{+\infty} f_i^{\text{inc}}(v) v dv}{\int_0^{+\infty} f_i^{\text{inc}}(v) dv} < \frac{(1-\alpha)}{(1+\alpha)} \sqrt{\frac{2}{\mu\pi}}, \tag{13}$$

- the Bohm criterion

$$B_\alpha(f_i^{\text{inc}}) := \frac{m_\alpha(0) + m'_\alpha(0)}{m_\alpha(0)} - \frac{\int_0^{+\infty} \frac{f_i^{\text{inc}}(v)}{v^2} dv}{\int_0^{+\infty} f_i^{\text{inc}}(v) dv} > 0, \tag{14}$$

where

$$\forall u \in [\phi_{\text{wall}}, 0], \quad m_\alpha(u) := 2 - (1-\alpha)\text{erfc}(\sqrt{u - \phi_{\text{wall}}}), \tag{15}$$

then for all $0 < \nu < \nu^c$ where

$$\nu^c := -\phi_{\text{wall}} B_\alpha(f_i^{\text{inc}}) \left(\frac{\int_0^{+\infty} f_i^{\text{inc}}(v) dv}{\int_0^{+\infty} \frac{f_i^{\text{inc}}(v)}{v} dv} \right) > 0 \tag{16}$$

there exists $\varepsilon^* > 0$ such that for all $\varepsilon \geq \varepsilon^*$ the weak solutions to (1)-(11) have the following properties:

- a non negative charge density:

$$\forall x \in [0,1], \quad n_i(x) \geq n_e(x) > 0, \tag{17}$$

- a sufficiently decreasing electric potential:

$$\forall x \in [0,1], \quad \partial_x \phi(x) \leq -\frac{\nu}{B_\alpha(f_i^{\text{inc}})} \left(\frac{\int_0^{+\infty} \frac{f_i^{\text{inc}}(v)}{v} dv}{\int_0^{+\infty} f_i^{\text{inc}}(v) dv} \right) < 0. \tag{18}$$

When the collision frequency vanishes, that is $\nu = 0$, it is proven in [4] that provided the inequalities (13) and (14) still hold, the system (1)-(12) has for any $\varepsilon > 0$ a unique weak solution which again satisfies the inequalities (17) and (18). The proof relies on a equivalent reformulation of the system as a minimization problem. This approach additionally yields quantitative estimates as $\varepsilon \to 0$ for both the electric field $\partial_x \phi$ and the charge density $n_i - n_e$ which mathematically pertains to the presence so called Debye sheath [23] .

A very exhaustive literature about numerical methods to approximate kinetic plasma models is available. We refer for example to [5, 22, 11, 7, 16, 13, 10, 9] for Particle-In-Cell methods, Semi-Lagragian methods and Galerkin type methods. Convergence and stability analysis of these methods can be found in the mentioned references. In the specific context of plasma sheaths, some of these numerical methods have been used [29, 19, 21, 25] with their own specificity according to the model under consideration. We mention that non stationary based numerical methods are often more generic in a sense, and enable to avoid dealing with the delicate problem of selecting the boundary conditions that reproduce the physics of sheaths. They are however more time consuming and less robust since they may not reach the desired stationary solution. As far as the numerical difficulties are concerned, they are all related to the multi-scale nature of the plasma sheath formation. The main observed numerical difficulties are threefold. The first one stems from the need of a high spatial resolution due to the boundary layer that forms in the different regimes $\varepsilon \ll 1$ and $\nu \gg 1$. The second one comes from the relative difference in velocities between electrons and ions due to the small mass ratio $\mu \ll 1$. The third one is related to the numerical treatment of the boundary conditions (6)-(7) which need a specific interpolation procedure with ghost points outside the computational domain. These three numerical difficulties bring stringent stability conditions and prohibitive computational effort. We refer to [21, 18] for numerical studies with physical parameters taken from the literature. Some cures are likely possible by following the so called Asymptotic-Preserving approach [17, 12] except for the numerical difficulties related to the presence of boundary layer which are not well-suited for this approach. Specific numerical methods must therefore be implemented in the context of plasma sheaths. The strategy followed in this work relies on the a priori knowledge of the mathematical structure of the solution. It is based on the analysis of the phase space by means of the characteristic curves. It is somehow very specific but it yields an exact integration of the transport equations (1)-(2) and thus no numerical error related to the transport equations is introduced. It provides a numerical method which has a strong analytical background.

The present work thus proposes a simple fixed point method to approximate the weak solutions of the boundary value problem (1)-(11). Our method takes fully advantage of the one dimensional structure of the model and follows closely the analysis developed in [3]. An exact integration of the transport equations (1)-(2) with the method of characteristics enables to have an exact representation of the densities f_i, f_e up to an error of approximation on ϕ. These exact formula are then used to compute the macroscopic densities and currents. It enables to reduce the two algebraic equations (10)-(11) to one single non linear equation to be solved for ϕ_{wall}. Once the couple $(n_0, \phi_{\text{wall}})$ is computed, the core of the method then consists in solving the non linear Poisson problem (3) with the boundary conditions (8) by a fixed point algorithm using a finite difference scheme. A suitable choice of the ions phase space discretization based on the geometry of the characteristics and convenient quadrature formulas for velocity integrals are proposed in order to ensure that the inequalities (17) and (18) are easily preserved at the discrete level which yields the stability of the method.

1.1. Summary of the numerical method

We now briefly summarize our method, it consists in the three following steps.

Step I - The method of characteristics for the Vlasov-Boltzmann equations. Following Section 4 of [3], provided $\phi \in W^{2,\infty}(0,1)$ is decreasing with $\phi(0) = 0$, the method of characteristics yields an explicit representation of the particles densities f_i and f_e as functions of the potential ϕ. Namely, integrating the Vlasov-Boltzmann equations (1)-(2) along the characteristics curves and using the boundary conditions (6)-(7), one obtains

$$\begin{aligned} f_i(x,v) = \mathbf{1}_{\{v>\sqrt{-2\phi(x)}\}}(x,v) f_i^{\text{inc}}\left(\sqrt{v^2+2\phi(x)}\right) \mathrm{e}^{\nu t_{\text{inc}}(x,v)} \\ + \mathbf{1}_{\{0<v<\sqrt{-2\phi(x)}\}}(x,v) \frac{-\nu \mathrm{e}^{\nu s_0(x,v)} n_i\left(\phi^{-1}(\phi(x)+v^2/2)\right)}{\partial_x \phi\left(\phi^{-1}(\phi(x)+v^2/2)\right)}. \end{aligned} \tag{19}$$

$$\begin{aligned} f_e(x,v) = n_0 \mathbf{1}_{\{v>\sqrt{\frac{2}{\mu}(\phi(x)-\phi(1))}\}}(x,v) f_e^{\text{inc}}\left(\sqrt{v^2-\frac{2}{\mu}\phi(x)}\right) \\ + n_0\alpha \mathbf{1}_{\{v<\sqrt{\frac{2}{\mu}(\phi(x)-\phi(1))}\}}(x,v) f_e^{\text{inc}}\left(\sqrt{v^2-\frac{2}{\mu}\phi(x)}\right). \end{aligned} \tag{20}$$

In (19), t_{inc} and s_0 are negative times given respectively by

$$t_{\text{inc}}(x,v) = -\int_0^x \frac{du}{\sqrt{v^2+2(\phi(x)-\phi(u))}}, \tag{21}$$

$$s_0(x,v) = -\int_{\phi^{-1}(\phi(x)+v^2/2)}^x \frac{du}{\sqrt{2(\phi(x)+v^2/2-\phi(u))}}. \tag{22}$$

Integrating with respect to the velocity $v \in \mathbb{R}$ both (19) and (20), one then obtains the following formulas for the macroscopic densities $n_i \equiv n_i[\phi]$ and $n_e \equiv n_e[\phi]$:

$$\begin{aligned} n_i[\phi](x) = \int_{\sqrt{-2\phi(x)}}^{+\infty} f_i^{\text{inc}}\left(\sqrt{v^2+2\phi(x)}\right) \mathrm{e}^{\nu t_{\text{inc}}(x,v)}\, dv \\ - \int_0^{\sqrt{-2\phi(x)}} \frac{\nu \mathrm{e}^{\nu s_0(x,v)} n_i[\phi](\phi^{-1}(\phi(x)+v^2/2))}{\partial_x \phi(\phi^{-1}(\phi(x)+v^2/2))}\, dv, \end{aligned} \tag{23}$$

$$n_e[\phi](x) = n_0 \mathrm{e}^{\phi(x)} m_\alpha\left(\phi(x)\right), \tag{24}$$

where m_α is given by (15). The ions density n_i solves an integral equation while the electrons density n_e is given explicitly. As for the current densities, they are given by

$$J_i = \int_0^{+\infty} f_i^{\text{inc}}(v) v dv, \tag{25}$$

$$J_e = n_0(1-\alpha)\sqrt{\frac{2}{\pi\mu}} e^{\phi_{\text{wall}}}. \tag{26}$$

Step II- Determination of the wall potential. Assuming $\phi(1) = \phi_{\text{wall}}$, the two algebraic equations (10) and (11) yields the equivalent system of unknown

$(n_0, \phi_{\text{wall}})$

$$\int_0^{+\infty} f_i^{\text{inc}}(v)dv = n_0 m_\alpha(0), \tag{27}$$

$$\int_0^{+\infty} f_i^{\text{inc}}(v)v dv = n_0(1-\alpha)\sqrt{\frac{2}{\pi\mu}} e^{\phi_{\text{wall}}}, \tag{28}$$

where we remind that $m_\alpha(0)$ is given by

$$m_\alpha(0) = 2 - (1-\alpha)\text{erfc}(\sqrt{-\phi_{\text{wall}}})$$

and thus also depends on ϕ_{wall}. Eliminating n_0 yields that ϕ_{wall} is the unique negative solution of the non linear equation

$$\mathcal{W}(\phi_{\text{wall}}) = 0 \tag{29}$$

where the function $\mathcal{W}$ is defined for $\varphi \leq 0$ by

$$\mathcal{W}(\varphi) = \big(2 - (1-\alpha)\text{erfc}(\sqrt{-\varphi})\big) \int_0^{+\infty} f_i^{\text{inc}}(v)v\, dv$$
$$-(1-\alpha)\sqrt{\frac{2}{\pi\mu}} \int_0^{+\infty} f_i^{\text{inc}}(v)\, dv e^{\varphi}. \tag{30}$$

The function $\mathcal{W}$ is continuous, decreasing and has a limit as $\varphi \to -\infty$ which is such that $\lim_{\varphi \to -\infty} \mathcal{W}(\phi) > 0$. Therefore the equation (29) has a unique negative solution if and only $\mathcal{W}(0) < 0$ which is the inequality (13). The equation (29) is then solved using a standard Newton method.

Step III-Solving the non linear Poisson problem. The non linear Poisson problem consists in finding a decreasing potential ϕ satisfying (18) such that

$$-\varepsilon^2 \partial_{xx}\phi(x) = n_i[\phi](x) - n_e[\phi](x), \qquad x \in [0,1], \tag{31}$$

$$\phi(0) = 0 \qquad \text{and} \qquad \phi(1) = \phi_{\text{wall}} < 0, \tag{32}$$

where $n_i[\phi] > 0$ solves the integral equation (23), $n_e[\phi] > 0$ is given explicitly on ϕ by (24) and the solution ϕ must ensure the inequality (17). We note that in the case $\nu = 0$, the Poisson problem (31)-(32) reformulates as a minimization problem [4]. Since $\nu > 0$, $n_i[\phi]$ solves a non trivial integral equation (23). The Poisson problem (31)-(32) is a strongly non linear integro-differential equation. Our numerical method consists in solving (31) with a fixed point method. The stability of the method is ensured by the inequalities (17) and (18). Our main concern in the rest of the paper is the preservation of these inequalities at the discrete level.

1.2. Organization

The outline of the paper is as follows. In the next section, we define the numerical scheme to solve the non linear Poisson problem (23)-(24)-(31)-(32). We detail the discretization, paying a particular attention to the ions phase space discretization in order to avoid the computation of ϕ^{-1} involved in the definition of $n_i[\phi]$, given by (23) and in s_0 defined by (22). Then in Section 3 we establish the stability properties to be satisfied by the numerical scheme, namely the discrete analogue of inequalities (17) and (18). In Section 4, several numerical experiments that are performed in the scope of the analysis and an interpretation of the results is proposed. Some results going beyond our analysis are also given. Eventually, a short conclusion is given in Section 5.

2. The numerical scheme

In all the sequel, we shall assume that the incoming ions density f_i^{inc} : $(0, +\infty) \to \mathbb{R}^+$ is at least piecewise continuous so that the upcoming quadrature formulas make sense. Moreover, we assume $\phi_{\text{wall}} < 0$ to solve exactly or approximately the equation (29). We begin with introducing a uniform discretization of the interval $[0, 1]$ of size $\Delta x = 1/(N + 1)$ where $N + 1$ denotes the number of intervals of discretization so that $x_j = j\Delta x$ for $0 \le j \le N+1$. We denote ϕ_j the approximation of $\phi(x_j)$ while $n_i[\phi]_j$ and $n_e[\phi]_j$ respectively denote the approximations of $n_i[\phi](x_j)$ and $n_e[\phi](x_j)$.

To approximate the sequence $(\phi_j)_{0\le j\le N+1}$ with the boundary conditions given by

$$\phi_0 = 0 \quad \text{and} \quad \phi_{N+1} = \phi_{\text{wall}},$$

we use the following fixed point numerical procedure:

$$-\frac{\varepsilon^2}{\Delta x^2}\left(\phi_{j+1}^{n+1} - 2\phi_j^{n+1} + \phi_{j-1}^{n+1}\right) = n_i[\phi^n]_j - n_e[\phi^n]_j, \tag{33}$$

where the initial sequence $(\phi_j^0)_{0\le j\le N+1}$ must satisfy the boundary conditions

$$\phi_0^0 = 0 \quad \text{and} \quad \phi_{N+1}^0 = \phi_{\text{wall}}.$$

In view of the inequality (18), we also impose this initial sequence to verify for all $0 \le j \le N$

$$\frac{1}{\Delta x}\left(\phi_{j+1}^0 - \phi_j^0\right) \le M_\phi < 0, \tag{34}$$

where M_ϕ will be defined as an approximation of the right hand side in the inequality (18).

Regarding the definition of $n_i[\phi]_j$, to approximate $n_i[\phi](x_j)$ defined by (23), we shall introduce a suitable discretization of half the phase space $(0,1)\times[0,+\infty)$ that avoid the computation of ϕ^{-1} involved in (23). As in [3], one uses the characteristic curves. These are the curves of algebraic equation $\frac{v^2}{2}+\phi(x)=\text{const}$. They span the domain $(0,1)\times[0,+\infty)$ so that one has the natural decomposition

$$(0,1)\times[0,+\infty)=D_1\cup D_2,$$

with

$$D_1=\left\{(x,v)\in(0,1)\times[0,+\infty)\ :\ v>\sqrt{-2\phi(x)}\right\}, \tag{35}$$

$$D_2=\left\{(x,v)\in(0,1)\times[0,+\infty)\ :\ 0\le v\le\sqrt{-2\phi(x)}\right\}. \tag{36}$$

The domain D_1 corresponds to characteristic curves that originate from $x=0$ with positive velocities, namely

$$\forall(x,v)\in D_1,\ \exists v_0>0,\ \frac{v_0^2}{2}=\frac{v^2}{2}+\phi(x). \tag{37}$$

The domain D_2 corresponds to characteristic curves that crosses $v=0$, namely

$$\forall(x,v)\in D_2,\ \exists\, 0\le x_0<1,\ \phi(x_0)=\frac{v^2}{2}+\phi(x). \tag{38}$$

In particular for a given pair (x_j,v) where $x_j\in(0,1)$ is a grid point and $v\in[0,\sqrt{-2\phi(x_j)})$, the corresponding x_0 in (38) is solution of the equation

$$\phi(x_0)=\frac{v^2}{2}+\phi(x_j). \tag{39}$$

From a numerical perspective, the equation (39) is not convenient since ϕ may be replaced by an approximation which is only known on a discrete set. If one wants to solve (39), then one needs somehow an ad hoc reconstruction of ϕ. A way to circumvent this issue is to choose v in such a way that x_0 belongs to the grid $(x_k)_{0\le k\le N+1}$ so that the equation (39) is trivially solved. Namely, we define a discretization of the velocity interval which depends on the grid $(x_k)_{0\le k\le N+1}$ using the equation of the characteristics (39) (see Fig 1). In this regard, for $0\le v\le\sqrt{-2\phi_j}$ with a given j, we set

$$v_{j-k}^j=\sqrt{2(\phi_k-\phi_j)},\quad 0\le k\le j, \tag{40}$$

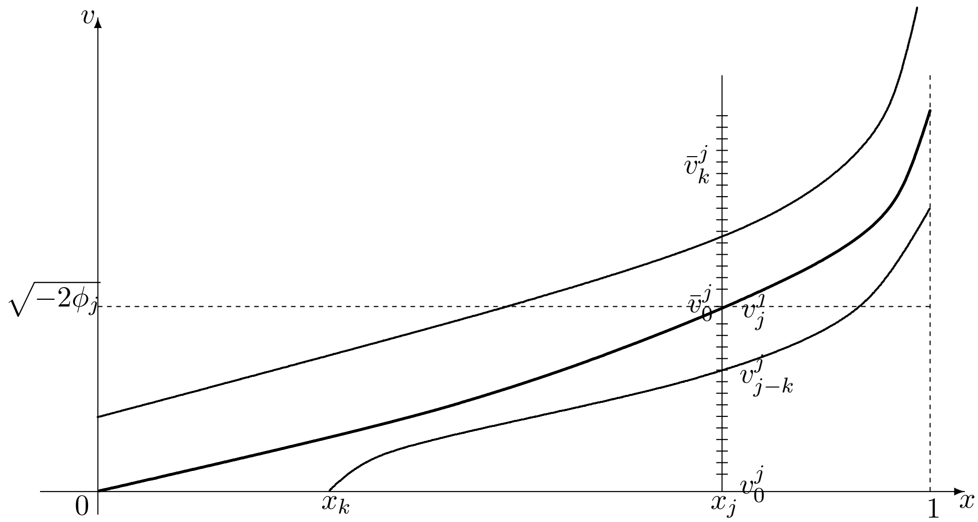

Figure 1: Schematic characteristics associated to the ions phase-space $(0,1)\times[0,+\infty)$ and its discretization. Solide lines represent some characteristic curves. For each grid point $0 < x_j < 1$, the velocity interval $[0,+\infty)$ is decomposed as $[0,+\infty) = [0,\sqrt{-2\phi(x_j)}] \cup (\sqrt{-2\phi(x_j)},+\infty)$. The interval $[0,\sqrt{-2\phi(x_j)}]$ is discretized with the grid $(v_{j-k}^j)_{0\leq k\leq j}$ and the interval $(\sqrt{-2\phi(x_j)},+\infty)$ is discretized with the grid $(\bar{v}_k^j)_{k\geq 0}$.

where $\phi_k - \phi_j \geq 0$ for all $0 \leq k \leq j$ provided $(\phi_j)_{0\leq j\leq N+1}$ satisfies

$$\frac{1}{\Delta x}\left(\phi_{j+1} - \phi_j\right) \leq M_\phi < 0. \tag{41}$$

For $v \geq \sqrt{-2\phi_j}$, we consider a uniform discretization of size $\Delta v > 0$ such that we set

$$\bar{v}_k^j = \sqrt{-2\phi_j} + k\Delta v, \qquad k \geq 0.$$

To avoid some possible confusion in the velocity discretization, we have denoted v_ℓ^j the discretization of v in $[0,\sqrt{-2\phi_j}]$ while $\bar{v}_\ell^j$ denotes the discretization of v in $[\sqrt{-2\phi_j},+\infty)$.

We need now to define an approximation of $n_i[\phi](x_j)$ for all $0 \leq j \leq N+1$. To do so, the integrals involved in (23) are approximated using the trapezoidal rules. More precisely, the first integral in (23) is approximated by $\mathcal{I}^\infty[\phi]_j$ for all $0 \le j \le N+1$ defined by

$$\mathcal{I}^\infty[\phi]_j = \sum_{k\ge 0} \frac{\Delta v}{2} \left(f_i^{\mathrm{inc}}\left(\sqrt{\left(\bar{v}_k^j\right)^2 + 2\phi_j}\right) \mathrm{e}^{\nu \bar{t}_{\mathrm{inc}}[\phi]\left(x_j, \bar{v}_k^j\right)} + f_i^{\mathrm{inc}}\left(\sqrt{\left(\bar{v}_{k+1}^j\right)^2 + 2\phi_j}\right) \mathrm{e}^{\nu \bar{t}_{\mathrm{inc}}[\phi]\left(x_j, \bar{v}_{k+1}^j\right)}\right) \tag{42}$$

where $\bar{t}_{\mathrm{inc}}[\phi]\left(x_j, \bar{v}_k^j\right)$ is an approximation of the time $t_{\mathrm{inc}}(x_j, \bar{v}_k^j)$ given in (21). It is defined by $\bar{t}_{\mathrm{inc}}[\phi]\left(x_0, \bar{v}_k^0\right) = 0$ and for $1 \le j \le N+1$ a midpoint rule is used:

$$\bar{t}_{\mathrm{inc}}[\phi]\left(x_j, \bar{v}_k^j\right) = -\sum_{\ell=0}^{j-1} \frac{\Delta x}{\sqrt{\left(\bar{v}_k^j\right)^2 + 2\phi_j - (\phi_\ell + \phi_{\ell+1})}}. \tag{43}$$

The second integral is approximated by $\mathcal{I}^0[\phi]_j$ with $\mathcal{I}^0[\phi]_0 = 0$ and for $1 \le j \le N+1$

$$\mathcal{I}^0[\phi]_j = \sum_{k=0}^{j-1} \frac{v_{j-(k+1)}^j - v_{j-k}^j}{2} \left(\nu \mathrm{e}^{\nu \bar{s}_0(x_j, v_{j-k}^j)} \frac{\overline{n_i[\phi]}(\phi^{-1}(\phi_j + (v_{j-k}^j)^2/2))}{\overline{\partial_x \phi}(\phi^{-1}(\phi_j + (v_{j-k}^j)^2/2))} + \nu \mathrm{e}^{\nu \bar{s}_0(x_j, v_{j-(k+1)}^j)} \frac{\overline{n_i[\phi]}(\phi^{-1}(\phi_j + (v_{j-(k+1)}^j)^2/2))}{\overline{\partial_x \phi}(\phi^{-1}(\phi_j + (v_{j-(k+1)}^j)^2/2))}\right)$$

where $\overline{n_i[\phi]}(\phi^{-1}(\phi_j + (v_{j-k}^j)^2/2))$, $\overline{\partial_x \phi}(\phi^{-1}(\phi_j + (v_{j-k}^j)^2/2))$ and $\bar{s}_0(x_j, v_{j-k}^j)$ are approximations of $n_i[\phi](\phi^{-1}(\phi_j + (v_{j-k}^j)^2/2))$, $\partial_x \phi(\phi^{-1}(\phi_j + (v_{j-k}^j)^2/2))$ and $s_0(x_j, v_{j-k}^j)$ given by (22). They are constructed using the velocity discretization defined by (40). Indeed, we have

$$\phi_j + \frac{(v_{j-k}^j)^2}{2} = \phi_k.$$

One therefore naturally defines,

$$\overline{n_i[\phi]}(\phi^{-1}(\phi_j + (v_{j-k}^j)^2/2)) = n_i[\phi]_k, \tag{44}$$

$$\overline{\partial_x \phi}(\phi^{-1}(\phi_j + (v_{j-k}^j)^2/2)) = \overline{\partial_x \phi}_k, \tag{45}$$

$$\bar{s}_0(x_j, v_{j-k}^j) = -\sum_{\ell=k}^{j-1} \frac{\Delta x}{\sqrt{2\left(\phi_k - \phi_{\ell+1}\right)}}, \tag{46}$$

where $\overline{\partial_x \phi_k}$ denotes an approximation of $\partial_x \phi(x_k)$ such that the control of the variations of $(\phi_j)_{0\le j\le N+1}$ through the inequality (41) also implies

$$\overline{\partial_x \phi_k} \le M_\phi < 0. \tag{47}$$

As a consequence, $\mathcal{I}^0[\phi]_j$ rewrites $\mathcal{I}^0[\phi]_0 = 0$ and for $1 \le j \le N+1$

$$\mathcal{I}^0[\phi]_j = \frac{\nu}{2}\sum_{k=0}^{j-1}\left(\sqrt{\phi_{k+1}-\phi_j} - \sqrt{\phi_k - \phi_j}\right) \times \left(\mathrm{e}^{\nu \bar{s}_0(x_j, v^j_{j-k})}\frac{n_i[\phi]_k}{\overline{\partial_x \phi_k}} + \mathrm{e}^{\nu \bar{s}_0(x_j, v^j_{j-(k+1)})}\frac{n_i[\phi]_{k+1}}{\overline{\partial_x \phi_{k+1}}}\right). \tag{48}$$

The approximation $n_i[\phi]_j$ is then defined by

$$n_i[\phi]_j = \mathcal{I}^\infty[\phi]_j + \mathcal{I}^0[\phi]_j. \tag{49}$$

For the proof of the stability properties (17) and (18), it is convenient to define several consistent approximations of the constant n_0 which is given according to equation (27) by

$$n_0 = \frac{1}{m_\alpha(0)}\int_0^{+\infty} f_i^{\mathrm{inc}}(v)dv.$$

The trick is to remark that for all $\varphi < 0$ we have

$$\int_0^{+\infty} f_i^{\mathrm{inc}}(v)\, dv = \int_{\sqrt{-2\varphi}}^{+\infty} f_i^{\mathrm{inc}}(\sqrt{v^2+2\varphi})\frac{v}{\sqrt{v^2+2\varphi}}\, dv,$$

so that n_0 can also be expressed in terms of the sequence $(\phi_j)_{0\le j\le N+1}$ as

$$n_0 = \frac{1}{m_\alpha(0)}\int_{\sqrt{-2\phi_j}}^{+\infty} f_i^{\mathrm{inc}}(\sqrt{v^2+2\phi_j})\frac{v}{\sqrt{v^2+2\phi_j}}\, dv.$$

One can thus define an approximation of n_0 for each ϕ_j by

$$n_0^j m_\alpha(0) = \sum_{k\ge 0}\frac{\Delta v}{2}\left(f_i^{\mathrm{inc}}(\sqrt{(\bar{v}^j_k)^2+2\phi_j})\frac{\bar{v}^j_k}{\sqrt{(\bar{v}^j_k)^2+2\phi_j}} + f_i^{\mathrm{inc}}(\sqrt{(\bar{v}^j_{k+1})^2+2\phi_j})\frac{\bar{v}^j_{k+1}}{\sqrt{(\bar{v}^j_{k+1})^2+2\phi_j}}\right). \tag{50}$$

The full sequence $(n_0^j)_{0\leq j\leq N+1}$ is of course consistent with the constant n_0 defined by (27).

As for $n_e[\phi]_j$, we simply define

$$n_e[\phi]_j = n_0^j \mathrm{e}^{\phi_j} m_\alpha(\phi_j). \tag{51}$$

The definition of the scheme is now achieved. Before we turn to the study of the stability properties satisfied by this scheme, it is worth noticing that $n_i[\phi]_j$ is solution of a $(N+2)\times(N+2)$ triangular linear system in the form

$$n_i[\phi] = \mathcal{I}^\infty + M \cdot n_i[\phi], \tag{52}$$

where $n_i[\phi] \in \mathbb{R}^{N+2}$ is the unknown vector made of $(n_i[\phi]_j)_{0\leq j\leq N+1}$, $\mathcal{I}^\infty \in \mathbb{R}^{N+2}$ is the vector with components $(\mathcal{I}^\infty[\phi]_j)_{0\leq j\leq N+1}$ and M is a triangular matrix of size $N+2$ such that for $0 \leq j \leq N+1$

$$(M \cdot n_i[\phi])_i = \mathcal{I}^0[\phi]_j. \tag{53}$$

3. Stability properties

We consider the scheme (33),(49),(51) to approximate the solutions of (1)-(12). One has to prove the discrete analogue of the inequalities (17) and (18) that reads

$$\begin{aligned}
&\frac{1}{\Delta x}\left(\phi_{j+1}^n - \phi_j^n\right) \leq M_\phi < 0,\\
&n_i[\phi^n]_j - n_e[\phi^n]_j \geq 0,
\end{aligned}$$

during all the fixed point iterations $n \in \mathbb{N}$ where M_ϕ will be defined as an approximation of the right hand side in the inequality (18). In this regard, we introduce the critical re-emission coefficient

$$\alpha_c := \frac{1-\sqrt{\frac{\pi\mu}{2}}}{1+\sqrt{\frac{\pi\mu}{2}}} \tag{54}$$

which for all the physical mass ratio μ such that $0 < \alpha_c < 1$. Then our main result is the following.

Theorem 3.1. *Let $\alpha \in [0, \alpha_c]$. Assume f_i^{inc} satisfies (13) so that the pair $(n_0, \phi_{\mathrm{wall}}) \in (0, +\infty)\times(-\infty, 0)$ is uniquely determined by (27)-(28). Assume moreover the following discrete Bohm criterion : for all $0 \leq j \leq N+1$*

$$\bar{B}^j_\alpha(f^{\text{inc}}_i) = \frac{m_\alpha(0) + m'_\alpha(0)}{m_\alpha(0)} - \frac{I^j_2}{I^j_0} > 0 \tag{55}$$

where I^j_0 and I^j_1 are given by (63). Let $(\phi^0_\ell)_{0\le\ell\le N+1}$ be a given sequence such that $\phi^0_0 = 0$, $\phi^0_{N+1} = \phi_{\text{wall}} < 0$ and $(\phi^0_{\ell+1} - \phi^0_\ell)/\Delta x \le M_\phi < 0$ for all $0 \le \ell \le N$ where M_ϕ is given by (64). Then for all $\nu > 0$ such that

$$-\phi_{\text{wall}} > \max_{0\le j\le N+1} \left(\frac{\nu I^j_1}{\bar{B}^j_\alpha(f^{\text{inc}}_i) I^j_0} \right), \tag{56}$$

there exists $\varepsilon^\star > 0$, such that for all $\varepsilon \ge \varepsilon^\star$, the updated sequence $(\phi^{n+1}_\ell)_{0\le\ell\le N+1}$ defined by the scheme (33),(49),(51) with the boundary conditions

$$\phi^{n+1}_0 = 0 \quad \text{and} \quad \phi^{n+1}_{N+1} = \phi_{\text{wall}} < 0. \tag{57}$$

verifies during all the iterations $n \in \mathbb{N}$:

$$n_i[\phi^n]_j - n_e[\phi^n]_j \ge 0, \quad 0 \le j \le N+1, \tag{58}$$

$$\frac{1}{\Delta x}(\phi^n_{j+1} - \phi^n_j) \le M_\phi, \quad 0 \le j \le N. \tag{59}$$

To prove this result, we shall need several discrete a priori estimates that are the focus of the next section.

3.1. A priori estimates

The first one is an estimate of $\bar{t}_{\text{inc}}[\phi]$.

Lemma 3.2. *Let $(\phi_\ell)_{0\le\ell\le N+1}$ be a given sequence such that*

$$\phi_0 = 0 \quad \text{and} \quad \frac{1}{\Delta x}(\phi_{\ell+1} - \phi_\ell) \le M_\phi, \tag{60}$$

where $M_\phi < 0$ is a given constant which may eventually depend on the parameters of the model and ϕ_{wall}. Then for $0 \le j \le N+1$, we have

$$\bar{t}_{\text{inc}}[\phi](x_j, \bar{v}^j_k) \ge \frac{1}{M_\phi} \left(\bar{v}^j_k - \sqrt{(\bar{v}^j_k)^2 + 2\phi_j} \right), \tag{61}$$

where $\bar{t}_{\text{inc}}$ is defined by (43).

Proof. With $\bar{t}_{\text{inc}}[\phi](x_j, \bar{v}_k^j)$ given by (43), we write

$$\bar{t}_{\text{inc}}[\phi](x_j, \bar{v}_k^j) = \sum_{\ell=0}^{j-1} \frac{1}{(\phi_{\ell+1} - \phi_\ell)/\Delta x} \frac{1}{\sqrt{(\bar{v}_k^j)^2 + 2\phi_j - (\phi_\ell + \phi_{\ell+1})}} (\phi_\ell - \phi_{\ell+1}).$$

Since $(\phi_\ell)_{0 \leq \ell \leq N+1}$ is imposed to satisfy (60), we get

$$\bar{t}_{\text{inc}}[\phi](x_j, \bar{v}_k^j) \geq \frac{1}{M_\phi} \sum_{\ell=0}^{j-1} \frac{1}{\sqrt{(\bar{v}_k^j)^2 + 2\phi_j - (\phi_\ell + \phi_{\ell+1})}} (\phi_\ell - \phi_{\ell+1}).$$

Let us emphasize that the function $\varphi \leq 0 \mapsto g(\varphi) = 1/\sqrt{(\bar{v}_k^j)^2 + 2\phi_j - 2\varphi}$ is well defined since $(\bar{v}_k^j)^2 + 2\phi_j \geq 0$ and convex. As a consequence, for all $\phi_{\ell+1} < \varphi < \phi_\ell$ we have

$$g\left(\frac{\phi_\ell + \phi_{\ell+1}}{2}\right) + \left(\varphi - \frac{\phi_\ell + \phi_{\ell+1}}{2}\right) g'\left(\frac{\phi_\ell + \phi_{\ell+1}}{2}\right) \leq g(\varphi).$$

By integrating the above relation with respect of φ over $[\phi_{\ell+1}, \phi_\ell]$, we obtain

$$(\phi_\ell - \phi_{\ell+1}) g\left(\frac{\phi_\ell + \phi_{\ell+1}}{2}\right) \leq \int_{\phi_{\ell+1}}^{\phi_\ell} g(\varphi)\, d\varphi,$$

that re-writes

$$\frac{\phi_\ell - \phi_{\ell+1}}{\sqrt{(\bar{v}_k^j)^2 + 2\phi_j - (\phi_\ell + \phi_{\ell+1})}} \leq \int_{\phi_{\ell+1}}^{\phi_\ell} \frac{d\varphi}{\sqrt{(\bar{v}_k^j)^2 + 2\phi_j - 2\varphi}}.$$

As a consequence, we have the following sequence of inequalities (M_ϕ being negative):

$$\begin{aligned}
\bar{t}_{\text{inc}}[\phi](x_j, \bar{v}_k^j) &\geq \frac{1}{M_\phi} \sum_{\ell=0}^{j-1} \int_{\phi_{\ell+1}}^{\phi_\ell} \frac{d\varphi}{\sqrt{(\bar{v}_k^j)^2 + 2\phi_j - 2\varphi}} \\
&\geq \frac{1}{M_\phi} \int_{\phi_j}^{0} \frac{d\varphi}{\sqrt{(\bar{v}_k^j)^2 + 2\phi_j - 2\varphi}} \\
&\geq \frac{1}{M_\phi} \left(\bar{v}_k^j - \sqrt{(\bar{v}_k^j)^2 + 2\varphi_j} \right).
\end{aligned}$$

□

Using the estimate of $\bar{t}_{\rm inc}$, given by (61), we now establish that $n_i[\phi]_j - n_e[\phi]_j$ stays non-negative.

Lemma 3.3. *Let us introduce*

$$\bar{w}_k^j = \sqrt{(\bar{v}_k^j)^2 + 2\phi_j}, \tag{62}$$

so that $\bar{v}_k^j = \sqrt{(\bar{w}_k^j)^2 - 2\phi_j}$. *Let us set for* $0 \le j \le N+1$

$$I_\delta^j = \sum_{k\ge 0} \frac{\Delta v}{2}\left(f_i^{inc}(\bar{w}_k^j)\frac{\bar{v}_k^j}{(\bar{w}_k^j)^{\delta+1}} + f_i^{inc}(\bar{w}_{k+1}^j)\frac{\bar{v}_{k+1}^j}{(\bar{w}_{k+1}^j)^{\delta+1}}\right). \tag{63}$$

Assume the discrete Bohm criterion (55). *Let* $(\phi_\ell)_{0\le \ell\le N+1}$ *be a given sequence such that (60) holds for a constant* M_ϕ *defined as follows:*

$$M_\phi = -\max_{0\le j\le N+1}\left(\frac{\nu}{\bar{B}_\alpha^j(f_i^{\rm inc})}\frac{I_1^j}{I_0^j}\right). \tag{64}$$

With Δx *small enough, we have for all* $0 \le j \le N+1$

$$n_i[\phi]_j - n_e[\phi]_j \ge 0, \tag{65}$$

where $n_i[\phi]_j$ *and* $n_e[\phi]_j$ *are defined by (49) and (51).*

We underline that $\bar{B}_\alpha^j(f_i^{\rm inc})$, defined by (55), is nothing but the discrete version of the Bohm number given by (14). Indeed, for all $0 \le j \le N+1$, the quantities I_δ^j are easily shown to be consistent with

$$\int_{\sqrt{-2\phi_j}}^{+\infty} f_i^{\rm inc}(\sqrt{v^2+2\phi_j})\frac{v}{(\sqrt{v^2+2\phi_j})^{\delta+1}}\,dv = \int_0^{+\infty} f_i^{\rm inc}(w)\frac{dw}{w^\delta},$$

so that the consistency with $B_\alpha(f_i^{\rm inc})$ holds. We now prove the Lemma 3.3.

Proof. First, we notice that $n_i[\phi]_j$ for all $0 \le j \le N+1$ is non-negative provided Δx is small enough. Indeed, $n_i[\phi]_j$ is defined by (49) which reformulates as a triangular linear system (52) in the form

$$(\mathrm{I_d} - M)\cdot n_i[\phi] = \mathcal{I}^\infty,$$

where $\mathrm{I_d}$ stands for the identity matrix in $\mathbb{R}^{N+2}\times\mathbb{R}^{N+2}$. We easily remark that all the non-diagonal components of the triangular matrix $\mathrm{I_d} - M$ are non-positive. Moreover, the diagonal components of M are negative defined by

$$M_{jj} = -\frac{\sqrt{\phi_{j-1} - \phi_j}}{\overline{\partial_x \phi_j}} \mathrm{e}^{\nu \bar{s}_0(x_j, v_0^j)},$$

so that $M_{jj} = \mathcal{O}(\sqrt{\Delta x})$. Then, $1 - M_{jj} > 0$ provided Δx is small enough. As a consequence, we deduce that $n_i[\phi]_j \geq 0$ for all $0 \leq j \leq N+1$.

Now, since $n_i[\phi]_j \geq 0$, we immediately obtain $\mathcal{I}^0[\phi]_j \geq 0$ for all $0 \leq j \leq N+1$. Then, it is sufficient to establish $\mathcal{I}^\infty[\phi]_j - n_e[\phi]_j \geq 0$ for all $0 \leq j \leq N+1$ to get the estimate (65). One remarks that with $\mathcal{I}^\infty[\phi]_j$ defined by (42) and $n_e[\phi]_j$ by (51), we have for all $0 \leq j \leq N+1$

$$\mathcal{I}^\infty[\phi]_j - n_e[\phi]_j = \mathrm{e}^{\phi_j} \left(\sum_{k \geq 0} \frac{\Delta v}{2} \left(f_i^{\mathrm{inc}}(\bar{w}_k^j) \mathrm{e}^{-\phi_j + \nu \bar{t}_{\mathrm{inc}}(x_j, \bar{v}_k^j)} + f_i^{\mathrm{inc}}(\bar{w}_{k+1}^j) \mathrm{e}^{-\phi_j + \nu \bar{t}_{\mathrm{inc}}(x_j, \bar{v}_{k+1}^j)} \right) - n_0^j m_\alpha(\phi_j) \right),$$

where $\bar{w}_k^j$ are defined by (62). Because of the estimate (61), we get

$$\mathcal{I}^\infty[\phi]_j - n_e[\phi]_j \geq \mathrm{e}^{\phi_j} \left(\sum_{k \geq 0} \frac{\Delta v}{2} \left(f_i^{\mathrm{inc}}(\bar{w}_k^j) \mathrm{e}^{-\phi_j + \frac{\nu}{M_\phi}(\bar{v}_k^j - \bar{w}_k^j)} + f_i^{\mathrm{inc}}(\bar{w}_{k+1}^j) \mathrm{e}^{-\phi_j + \frac{\nu}{M_\phi}(\bar{v}_{k+1}^j - \bar{w}_{k+1}^j)} \right) - n_0^j m_\alpha(\phi_j) \right). \tag{66}$$

We now use the following convexity inequality which is a consequence of the inequality (61) of Lemma 6.2 of [3] :

$$\mathrm{e}^{-\phi_j + \frac{\nu}{M_\phi}(\bar{v}_k^j - \bar{w}_k^j)} \geq \frac{\bar{v}_k^j}{\bar{w}_k^j} + \phi_j \bar{v}_k^j \left(\frac{1}{(\bar{w}_k^j)^3} - \frac{1}{\bar{w}_k^j} - \frac{\nu}{M_\phi} \frac{1}{(\bar{w}_k^j)^2} \right). \tag{67}$$

Since the function $\varphi \in (-\infty, 0] \mapsto m_\alpha(\varphi)$ is a concave function, we have

$$m_\alpha(\phi_j) \leq m_\alpha(0) + \phi_j m'_\alpha(0).$$

Gathering the above inequality and (67), we glean from (66) the following estimate:

$$\mathcal{I}^\infty[\phi]_j - n_e[\phi]_j \geq e^{\phi_j}\left(\sum_{k\geq 0}\frac{\Delta v}{2}\left(f_i^{\rm inc}(\bar w_k^j)\frac{\bar v_k^j}{\bar w_k^j}\alpha_k^j + f_i^{\rm inc}(\bar w_{k+1}^j)\frac{\bar v_{k+1}^j}{\bar w_{k+1}^j}\alpha_{k+1}^j\right)\right.$$
$$\left. - n_0^j m_\alpha(0) - n_0^j\phi_j m_\alpha'(0)\right),$$

where we have set

$$\alpha_k^j = 1 + \phi_j\left(\frac{1}{(\bar w_k^j)^2} - 1 - \frac{\nu}{M_\phi}\frac{1}{\bar w_k^j}\right).$$

Using the definition of n_0^j given by (50), we obtain

$$\mathcal{I}^\infty[\phi]_j - n_e[\phi]_j \geq \phi_j e^{\phi_j}\left(\sum_{k\geq 0}\frac{\Delta v}{2}\left(f_i^{\rm inc}(\bar w_k^j)\frac{\bar v_k^j}{\bar w_k^j}\beta_k^j + f_i^{\rm inc}(\bar w_{k+1}^j)\frac{\bar v_{k+1}^j}{\bar w_{k+1}^j}\beta_{k+1}^j\right)\right.$$
$$\left. - n_0^j(m_\alpha(0) + m_\alpha'(0))\right),$$

where we have set

$$\beta_k^j = \frac{1}{(\bar w_k^j)^2} - \frac{\nu}{M_\phi}\frac{1}{\bar w_k^j}.$$

With I_0^j, I_1^j and I_2^j defined by (63), we have

$$\mathcal{I}^\infty[\phi]_j - n_e[\phi]_j \geq \phi_j e^{\phi_j}\left(I_2^j - \frac{\nu}{M_\phi}I_1^j - n_0^j(m_\alpha(0) + m_\alpha'(0))\right).$$

According to (50), we have $n_0^j = I_0^j/m_\alpha(0)$ so that $\mathcal{I}^\infty[\phi]_j - n_e[\phi]_j \geq 0$ if M_ϕ satisfies (64). The proof is thus completed. □

In order to establish the control of the discrete variation of the sequence $(\phi_j)_{0\leq j\leq N+1}$ (18), we have to establish a uniform (with respect to ϕ_j) upper-bound for $n_i[\phi]_j$.

Lemma 3.4. *Let $(\phi_\ell)_{0\leq\ell\leq N+1}$ be a given sequence such that $\phi_0 = 0$, $\phi_{N+1} = \phi_{\rm wall} < 0$ and $(\phi_{\ell+1} - \phi_\ell)/\Delta x \leq M_\phi < 0$ for all $0 \leq \ell \leq N$ where M_ϕ verifies (64). Then, there exists a constant $\tau > 0$ independent of M_ϕ such that the following estimate holds for all $0 \leq j \leq N$:*

$$\frac{1}{2}(n_i[\phi]_j + n_i[\phi]_{j+1}) \leq 2e^{-\tau\frac{\phi_j+\phi_{j+1}}{2}}\min_{0\leq j\leq N+1} I_0^j, \tag{68}$$

where $n_i[\phi]_j$ is given by (49) and I_0^j is defined by (63).

Proof. We use the triangular linear system (52), given by

$$(\mathrm{Id} - M) \cdot n_i[\phi] = \mathcal{I}^\infty,$$

to determine the unknown vector $n_i[\phi] \in \mathbb{R}^{N+2}$. We consider a vectorial norm in $\mathbb{R}^{N+2}$ as follows:

$$\|V\|_\tau := \max_{0\le j\le N} \left(\frac{1}{2}(|V_j| + |V_{j+1}|) \mathrm{e}^{\tau \frac{\phi_j+\phi_{j+1}}{2}} \right),$$

where $\tau > 0$ is a constant to be defined.

First, we establish that there exists $\tau > 0$, large enough and independent of M_ϕ, such that we have for all $V \in \mathbb{R}^{N+2}$

$$\frac{1}{2}\left(|(M\cdot V)_j| + |(M\cdot V)_{j+1}|\right) \mathrm{e}^{\tau\frac{\phi_j+\phi_{j+1}}{2}} \le \frac{1}{2}\|V\|_\tau, \qquad 0 \le j \le N. \tag{69}$$

To address such an issue, we need a suitable estimate of $|(M\cdot V)_j|$. Since we have (53), with $(M\cdot V)_0 = 0$ we easily get for $1 \le j \le N+1$

$$\begin{aligned}|(M\cdot V)_j| \le & \frac{\nu}{\sqrt{2}} \sum_{k=0}^{j-1} \left| \sqrt{\phi_{k+1}-\phi_j} - \sqrt{\phi_k - \phi_j} \right| \times \\ & \left(\mathrm{e}^{\nu \bar{s}_0(x_j, v^j_{j-k})} \frac{|V_k|}{|\overline{\partial_x \phi}_k|} + \mathrm{e}^{\nu \bar{s}_0(x_j, v^j_{j-(k+1)})} \frac{|V_{k+1}|}{|\overline{\partial_x \phi}_{k+1}|} \right),\end{aligned}$$

where $\bar{s}_0(x_j, v^j_{j-k})$, given by (46) is negative. As a consequence, the above inequality rewrites

$$|(M\cdot V)_j| \le \frac{\nu}{\sqrt{2}} \sum_{k=0}^{j-1} \left| \sqrt{\phi_{k+1}-\phi_j} - \sqrt{\phi_k - \phi_j} \right| \times \left(\frac{|V_k|}{|\overline{\partial_x \phi}_k|} + \frac{|V_{k+1}|}{|\overline{\partial_x \phi}_{k+1}|} \right).$$

According to (47), with $(\phi_\ell)_{0\le \ell\le N+1}$ a decreasing sequence, we obtain

$$\begin{aligned}|(M\cdot V)_j| &\le \frac{\nu}{2|M_\phi|} \sum_{k=0}^{j-1} \left(\sqrt{2(\phi_k-\phi_j)} - \sqrt{2(\phi_{k+1}-\phi_j)} \right) (|V_k| + |V_{k+1}|) \\ &\le \frac{\nu}{2|M_\phi|} \sum_{k=0}^{j-1} \left(\sqrt{2(\phi_k-\phi_j)} - \sqrt{2(\phi_{k+1}-\phi_j)} \right) (|V_k| + |V_{k+1}|)\mathrm{e}^{\tau\frac{\phi_k+\phi_{k+1}}{2}} \mathrm{e}^{-\tau\frac{\phi_k+\phi_{k+1}}{2}} \\ &\le \frac{\nu}{|M_\phi|} \|V\|_\tau \sum_{k=0}^{j-1} \left(\sqrt{2(\phi_k-\phi_j)} - \sqrt{2(\phi_{k+1}-\phi_j)} \right) \mathrm{e}^{-\tau\frac{\phi_k+\phi_{k+1}}{2}},\end{aligned}$$

so that we get for $1 \leq j \leq N$

$$|(M \cdot V)_j| \leq \frac{\nu}{|M_\phi|} \|V\|_\tau \mathcal{S}_j, \tag{70}$$

where we have set for $1 \leq j \leq N+1$

$$\mathcal{S}_j = \sum_{k=0}^{j-1} \left(\sqrt{2(\phi_k - \phi_j)} - \sqrt{2(\phi_{k+1} - \phi_j)} \right) \mathrm{e}^{-\tau \frac{\phi_k + \phi_{k+1}}{2}}.$$

In order to obtain the expected inequality (69), we give an estimate satisfied by $\mathcal{S}_j$. Indeed, we have for $1 \leq j \leq N+1$

$$\mathcal{S}_j = \sum_{k=0}^{j-1} \frac{\sqrt{2(\phi_k - \phi_j)} - \sqrt{2(\phi_{k+1} - \phi_j)}}{\phi_k - \phi_{k+1}} \mathrm{e}^{-\tau \frac{\phi_k + \phi_{k+1}}{2}} (\phi_k - \phi_{k+1}).$$

Let consider $p > 0$ and $q > 0$ such that $\frac{1}{p} + \frac{1}{q} = 1$. Then using the Holder inequality, we get

$$\mathcal{S}_j \leq \left(\sum_{k=0}^{j-1} \mathrm{e}^{-q\tau \frac{\phi_k + \phi_{k+1}}{2}} (\phi_k - \phi_{k+1}) \right)^{\frac{1}{q}} \times$$
$$\left(\sum_{k=0}^{j-1} \left(\frac{\sqrt{2(\phi_k - \phi_j)} - \sqrt{2(\phi_{k+1} - \phi_j)}}{\phi_k - \phi_{k+1}} \right)^p (\phi_k - \phi_{k+1}) \right)^{\frac{1}{p}}.$$

Notice that

$$\mathrm{e}^{-q\tau \frac{\phi_k + \phi_{k+1}}{2}} (\phi_k - \phi_{k+1}) \leq \int_{\phi_{k+1}}^{\phi_k} \mathrm{e}^{-q\tau\varphi} \, d\varphi,$$

so that we have, since $\phi_0 = 0$,

$$\begin{aligned} \sum_{k=0}^{j-1} \mathrm{e}^{-q\tau \frac{\phi_k + \phi_{k+1}}{2}} (\phi_k - \phi_{k+1}) &\leq \int_{\phi_j}^{0} \mathrm{e}^{-q\tau\varphi} \, d\varphi \\ &\leq \frac{1}{q\tau} \left(\mathrm{e}^{-q\tau\phi_j} - 1 \right). \end{aligned} \tag{71}$$

Moreover, we have

$$\frac{\sqrt{2(\phi_k - \phi_j)} - \sqrt{2(\phi_{k+1} - \phi_j)}}{\phi_k - \phi_{k+1}} = \frac{1}{\phi_k - \phi_{k+1}} \int_{\phi_{k+1}}^{\phi_k} \frac{d\varphi}{\sqrt{2(\varphi - \phi_j)}}.$$

Using Jensen's inequality, we then obtain

$$\left(\frac{\sqrt{2(\phi_k-\phi_j)}-\sqrt{2(\phi_{k+1}-\phi_j)}}{\phi_k-\phi_{k+1}}\right)^p \le \frac{1}{\phi_k-\phi_{k+1}}\int_{\phi_{k+1}}^{\phi_k}(2(\varphi-\phi_j))^{-\frac{p}{2}}\ d\varphi,$$

so that for $p<2$,

$$\begin{aligned}\sum_{k=0}^{j-1}\left(\frac{\sqrt{2(\phi_k-\phi_j)}-\sqrt{2(\phi_{k+1}-\phi_j)}}{\phi_k-\phi_{k+1}}\right)^p(\phi_k-\phi_{k+1}) &\le \int_{\phi_j}^{\phi_0}(2(\varphi-\phi_j))^{-\frac{p}{2}}\ d\varphi \\ &\le \frac{1}{2-p}(-2\phi_j)^{1-\frac{p}{2}}.\end{aligned} \tag{72}$$

Now, from (71) and (72), it results the following estimate of $\mathcal{S}_j$ for $1\le j\le N+1$:

$$\mathcal{S}_j \le \left(\frac{\mathrm{e}^{-q\tau\phi_j}-1}{q\tau}\right)^{\frac{1}{q}}\frac{(-2\phi_j)^{\frac{1}{p}-\frac{1}{2}}}{(2-p)^{\frac{1}{p}}}.$$

Since we have $\phi_{\text{wall}}\le\phi_{j+1}\le\phi_j\le 0$, then we get

$$\frac{1}{2}\left(\mathcal{S}_j+\mathcal{S}_{j+1}\right)\mathrm{e}^{\tau\frac{\phi_j+\phi_{j+1}}{2}} \le \frac{1}{(q\tau)^{\frac{1}{q}}}\left(\frac{(-2\phi_{\text{wall}})^{1-\frac{p}{2}}}{2-p}\right)^{\frac{1}{p}}.$$

As a consequence, it suffices to consider

$$\tau > \frac{1}{q}\left(2\left(\frac{(-2\phi_{\text{wall}})^{1-\frac{p}{2}}}{2-p}\right)^{\frac{1}{p}}\max_{0\le j\le N+1}\left(\bar{B}_\alpha^j(f_i^{\text{inc}})\frac{I_0^j}{I_1^j}\right)\right)^q,$$

where $\bar{B}_\alpha^j(f_i^{\text{inc}})$ is given by (55) and $I_{0,1}^j$ are defined by (63), to obtain for $0\le j\le N$

$$\frac{1}{2}\left(\mathcal{S}_j+\mathcal{S}_{j+1}\right)\mathrm{e}^{\tau\frac{\phi_j+\phi_{j+1}}{2}} \le \frac{1}{2}\min_{0\le j\le N+1}\left(\frac{1}{\bar{B}_\alpha^j(f_i^{\text{inc}})}\frac{I_1^j}{I_0^j}\right).$$

Involving (70) and the condition (64), we deduce the required estimate (69) where τ does not depend on M_ϕ.

The proof is easily completed since, from (69), we immediately obtain $\|M\|_\tau \le \frac{1}{2}$ so that

$$n_i[\phi] = \sum_{\ell\ge 0} M^\ell \mathcal{I}^\infty,$$

to write

$$\|n_i[\phi]\|_\tau \leq \|\mathcal{I}^\infty\|_\tau \sum_{\ell \geq 0} \|M\|_\tau^\ell \leq 2\|\mathcal{I}^\infty\|_\tau.$$

Next, with $\mathcal{I}^\infty[\phi]_j$ given by (42) and $\bar{t}_{\text{inc}}[\phi](x_j, \bar{v}_k^j) < 0$, we directly obtain $\mathcal{I}^\infty[\phi]_j \leq I_0^j$ for all $0 \leq j \leq N+1$ where I_0^j is given by (63). Moreover, since $\phi_{j+1} \leq \phi_j \leq 0$ then we have

$$\frac{1}{2}\left(I_j^\infty + I_{j+1}^\infty\right) \mathrm{e}^{\tau \frac{\phi_j + \phi_{j+1}}{2}} \leq \min_{0 \leq j \leq N+1} I_0^j,$$

so that

$$\|\mathcal{I}^\infty\|_\tau \leq \min_{0 \leq j \leq N+1} I_0^j.$$

As a consequence, $\|n_i[\phi]\|_\tau \leq 2 \min_{0 \leq j \leq N+1} I_0^j$ and we have

$$\begin{aligned}
\frac{1}{2}\left(n_i[\phi]_j + n_i[\phi]_{j+1}\right) &\leq \frac{1}{2}\left(n_i[\phi]_j + n_i[\phi]_{j+1}\right) \mathrm{e}^{\tau \frac{\phi_j + \phi_{j+1}}{2}} \mathrm{e}^{-\tau \frac{\phi_j + \phi_{j+1}}{2}} \\
&\leq \mathrm{e}^{-\tau \frac{\phi_j + \phi_{j+1}}{2}} \|n_i[\phi\|_\tau.
\end{aligned}$$

The proof is thus achieved. □

3.2. The proof of stability

We are now able to prove the Theorem 3.1.

Proof. By induction, both inequalities (58) and (59) are established provided that for a given sequence $(\phi_\ell)_{0 \leq \ell \leq N+1}$ such that $\phi_0^n = 0$, $\phi_{N+1}^n = \phi_{\text{wall}}$ and $(\phi_{\ell+1}^0 - \phi_\ell^0)/\Delta x \leq M_\phi$ for all $0 \leq \ell \leq N$, we prove (58) for ϕ^n and (59) for ϕ^{n+1}. The first estimate (58) for ϕ^n immediately comes from Lemma 3.3. Now, we have to show

$$\frac{1}{\Delta x}(\phi_{j+1}^{n+1} - \phi_j^{n+1}) \leq M_\phi. \tag{73}$$

To address such an issue, let us consider the summation of (33) from j equals one to ℓ, to write

$$-\frac{\varepsilon^2}{\Delta x}\left(\phi_{\ell+1}^{n+1} - \phi_\ell^{n+1} - \phi_1^{n+1} + \phi_0^{n+1}\right) = \sum_{j=1}^{\ell} \left(n_i[\phi^n]_j - n_e[\phi^n]_j\right) \Delta x. \tag{74}$$

By Lemma 3.3, we have $n_i[\phi^n]_j - n_e[\phi^n]_j \geq 0$ so that $\phi_{\ell+1}^{n+1} - \phi_\ell^{n+1} \leq \phi_1^{n+1} - \phi_0^{n+1}$. As a consequence, the required estimate (73) is established provided we prove

$$\frac{1}{\Delta x}(\phi_1^{n+1} - \phi_0^{n+1}) \leq M_\phi, \tag{75}$$

where we remind that

$$M_\phi = -\max_{0\le j\le N+1}\left(\frac{\nu I_1^j}{\bar{B}_\alpha^j(f_i^{\text{inc}})I_0^j}\right)$$

with $\bar{B}_\alpha^j(f_i^{\text{inc}})$ given by (55) and $I_{0,1}^j$ by (63).

In order to derive the above inequality, we sum (74) from ℓ equals from 0 to N, we then obtain

$$-\varepsilon^2\left((\phi_{N+1}^{n+1}-\phi_0^{n+1})-(N+1)(\phi_1^{n+1}-\phi_0^{n+1})\right)=\sum_{\ell=0}^{N}\sum_{j=1}^{\ell}\left(n_i[\phi]_j-n_e[\phi]_j\right)\Delta x^2.$$

Since $\Delta x = 1/(N+1)$, $\phi_0^{n+1} = 0$ and $\phi_{N+1}^{n+1} = \phi_{\text{wall}}$, the above relation reformulates as follows:

$$\frac{1}{\Delta x}\left(\phi_1^{n+1}-\phi_0^{n+1}\right)=\phi_{\text{wall}}+\frac{1}{\varepsilon^2}\sum_{\ell=0}^{N}\sum_{j=1}^{\ell}\left(n_i[\phi]_j-n_e[\phi]_j\right)\Delta x^2.$$

Now, the definition of $n_e[\phi]_j$ and the estimate (68) can be applied to get an upper bound of $n_i[\phi]_j - n_e[\phi]_j$. Indeed, we have for all $0\le j\le N$

$$\begin{aligned}
n_i[\phi]_j - n_e[\phi]_j &= \frac{1}{2}(n_i[\phi]_j+n_i[\phi]_{j+1})-n_e[\phi]_j+\frac{1}{2}(n_i[\phi]_j-n_i[\phi]_{j+1})\\
&\le 2\mathrm{e}^{-\tau\frac{\phi_j+\phi_{j+1}}{2}}\min_{0\le j\le N+1}(I_0^j)-\frac{I_0^j}{m_\alpha(0)}m_\alpha(\phi_j)\mathrm{e}^{\phi_j}+\frac{1}{2}(n_i[\phi]_j-n_i[\phi]_{j+1})\\
&\le C_{\text{wall}}+\frac{1}{2}(n_i[\phi]_j-n_i[\phi]_{j+1}),
\end{aligned}$$

where we have set

$$C_{\text{wall}}=\left(2\mathrm{e}^{-\tau\phi_{\text{wall}}}-\frac{m_\alpha(\phi_{\text{wall}})}{m_\alpha(0)}\mathrm{e}^{\phi_{\text{wall}}}\right)\min_{0\le j\le N+1}I_0^j.$$

Since $n_i[\phi]_j - n_e[\phi]_j > 0$ then $C_{wall} > 0$. As a consequence, we obtain

$$\begin{aligned}
\frac{1}{\Delta x}\left(\phi_1^{n+1}-\phi_0^{n+1}\right) &\le \phi_{\text{wall}}+\frac{1}{\varepsilon^2}\left(C_{wall}\frac{1-\Delta x}{2}+\frac{\Delta x^2}{2}\sum_{\ell=0}^{N}\sum_{j=1}^{\ell}(n_i[\phi]_j-n_i[\phi]_{j+1})\right)\\
&\le \phi_{\text{wall}}+\frac{1}{\varepsilon^2}\left(C_{wall}\frac{1-\Delta x}{2}+\frac{\Delta x^2}{2}\sum_{\ell=0}^{N}(n_i[\phi]_1-n_i[\phi]_{\ell+1})\right)\\
&\le \phi_{\text{wall}}+\frac{1}{\varepsilon^2}\left(C_{wall}\frac{1-\Delta x}{2}+\frac{\Delta x}{2}\max_{0\le j\le N}|n_i[\phi]_1-n_i[\phi]_{j+1}|\right).
\end{aligned}$$

The required inequality (75) is obtained for $\varepsilon \geq \varepsilon^\star$ where $\varepsilon^\star$ is given by

$$\varepsilon^\star = \max_{0\leq j\leq N+1}\left(\frac{1}{-\phi_{\text{wall}} - \frac{\nu I_1^j}{\bar{B}_\alpha^j(f_i^{\text{inc}})I_0^j}}\times \left(I_0^j \mathrm{e}^{-\tau\phi_{\text{wall}}} - \frac{I_0^j}{2m_\alpha(0)} m_\alpha(\phi_{\text{wall}})\mathrm{e}^{\phi_{\text{wall}}} + \mathcal{O}(\Delta x)\right)\right)^{\frac{1}{2}}. \quad (76)$$

The proof is then completed. □

4. Numerical experiments

This section is devoted to the numerical simulation of problem (1)-(12) in different regimes, using the numerical scheme presented in Section 2. Several studies are proposed. First, we consider a non collisional problem in Subsection 4.1 that is $\nu = 0$. We are able to compare our results with those of [4], so that this regime is seen as a validating case for our approach. Then, we are interested in collisional regimes in order to observe the influence of the collision frequency on the electrostatic potential ϕ and on the ionic and electronic distribution functions. In Subsection 4.2, we propose different numerical simulations compatible with hypotheses (13)-(14) and with a subcritical frequency $0 < \nu < \nu_c$. In this case, Theorem 3.1 holds (as well as its continuous version: Theorem 3.1 of [3]). Finally, we are interested in simulations that violate hypotheses of Theorem 3.1, in order to test our numerical scheme beyond the scope of this theorem. This numerical study is presented in Subsection 4.3.

In the simulations, we consider the following incoming functions

$$f_e^{inc}(v) = \sqrt{\frac{2\mu}{\pi}} e^{-\frac{\mu v^2}{2}},\ \forall v > 0, \quad (77)$$

$$f_i^{inc}(v) = \sqrt{\frac{2}{\pi}} v^2 e^{-\frac{v^2}{2}},\ \forall v > 0, \quad (78)$$

and the mass ratio of a Deuterium plasma $\mu = \frac{1}{3672}$, so that the critical re-emission coefficient $\alpha_c = \frac{1-\sqrt{(\pi\mu)/2}}{1+\sqrt{(\pi\mu)/2}} \approx 0.95$. We take $N+1 = 1000$ for the space discretization. The velocity domain for the computation of ion density is truncated to $[-8, 8]$ and domain D_1 is divided into 100 intervals.

We stop the fixed point method when two successive iterates k and $k+1$ are such that

$$\left\|\frac{\phi^{(k)} - \phi^{(k+1)}}{\phi^{(k)}}\right\|_\infty + \left\|\frac{(n_i - n_e)^{(k)} - (n_i - n_e)^{(k+1)}}{(n_i - n_e)^{(k)}}\right\|_\infty < 10^{-8}. \qquad (79)$$

Let us emphasize that the convergence of our fixed point method is not ensured for small values of ε. In practice, Theorem 3.1 implies the existence of $\varepsilon^\star > 0$ such that our fixed point algorithm converges for all $\varepsilon \geq \varepsilon^\star$, where the bound (76) is not optimal.

4.1. The non collisional sheath

We are first interested in a non collisional problem, with parameters $\nu = 0$, $\alpha = 0$. Admissibility condition (13) and Bohm criterion (14) are satisfied. A Newton iterative method solving (29) up to 10^{-16} gives $\phi_{\text{wall}} \approx -2.719$ and a density reference $n_0 \approx 0.505$. Here, we consider two values of ε: 1 and 0.2. We plot the electrostatic potential $\phi(x)$ in Figure 2 and the densities $n_i(x)$, $n_e(x)$ in Figure 3.

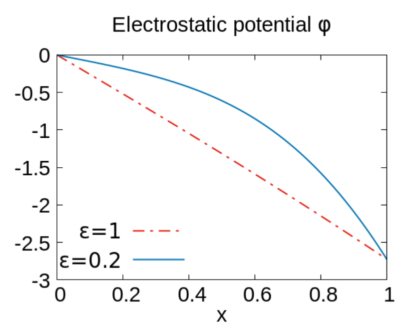

Figure 2: Electrostatic potential $\phi(x)$ for two values of ε: 1 and 0.2, in the non collisional regime $\nu = 0$, $\alpha = 0$.

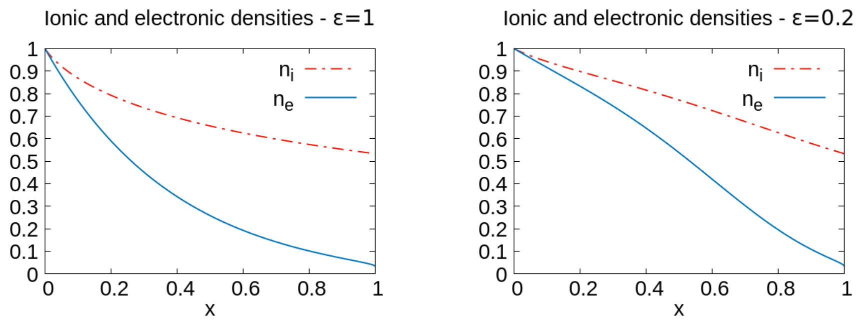

Figure 3: Ionic $n_i(x)$ and electronic $n_e(x)$ densities for two values of ε: 1 (left) and 0.2 (right), in the non collisional regime $\nu = 0$, $\alpha = 0$.

Then, we represent distribution functions: f_i in Figure 4 and f_e in Figure 5, for both values of ε (we propose two different views for each figure).

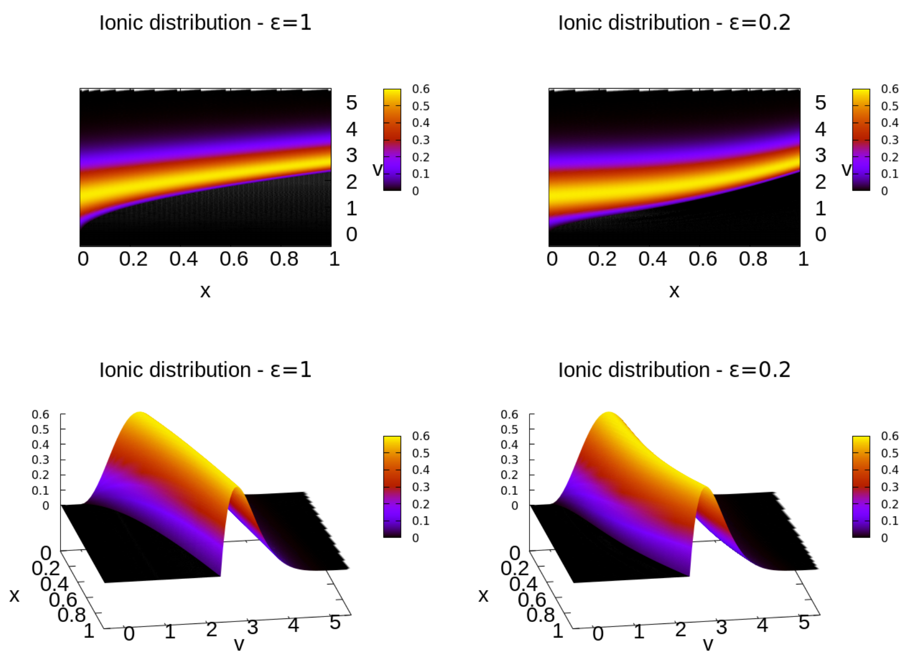

Figure 4: Ionic distribution function $f_i(x, v)$ for two values of ε: 1 (left) and 0.2 (right), in the non collisional regime $\nu = 0$, $\alpha = 0$. Two differents views on top and bottom.

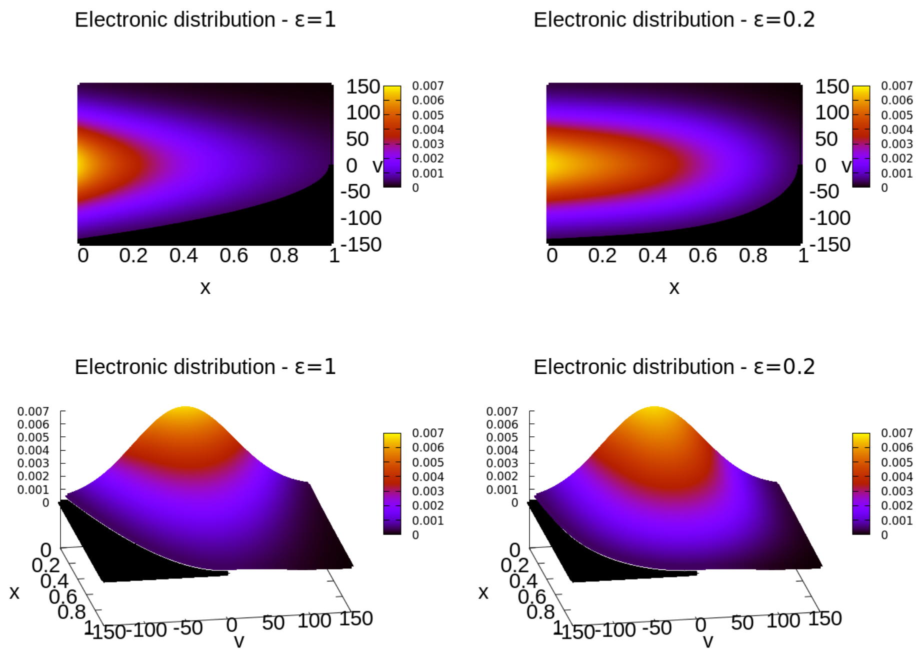

Figure 5: Electronic distribution function $f_e(x, v)$ for two values of ε: 1 (left) and 0.2 (right), in the non collisional regime $\nu = 0$, $\alpha = 0$. Two differents views on top and bottom.

These figures show the influence of ε and can be compared to numerical results proposed in [4]. We did not obtain convergence of our fixed point method for smaller values of ε. Even if our approach prevents us from taking small values of ε, it presents the good behavior. The numerical scheme presented in [4] is valid for smaller values of ε, but is specific to the non collisional case $\nu = 0$. It is based on the minimization formulation of the non linear Poisson problem. In the collisional case $\nu > 0$, such an approach cannot be applied directly because the non linear Poisson problem (3) does not reformulate as a minimization problem. The difficulty stems from the integral equation satisfied by n_i (23).

4.2. Collisional problems in the scope of Theorem 3.1

We are now interested in collisional problem staying in the scope of the numerical analysis done in this paper, and in particular $0 < \nu < \nu_c$ where the critical collisional frequency is defined by (16). We study the influence of physical parameters ν, α and ε.

We point out that Theorem 3.1 ensures the existence of $\varepsilon^\star$ such that the numerical scheme preserves the physical properties (58) and (59) for all $\varepsilon \geq \varepsilon^\star$.The value of $\varepsilon^\star$ given by (76) is in practice not optimal. In the numerical approach, we define the minimal value $\varepsilon^{min} \leq \varepsilon^\star$ for which we are able to make the fixed point method converge. The convergence depends on the initial iterate, that is why we have implemented a numerical continuation method over ε. If the fixed point method converges for a value of ε, we use the obtained $\phi[\varepsilon]$ as initial guess for the algorithm with $\varepsilon - 0.001$ and we continue until the fixed point method diverges. The smallest value for which we have convergence is denoted as ε^{min}. The step 0.001 is chosen as a compromise between precision on ε^{min} and computational time.

On the one hand, we fix $\alpha = 0$, so that the theoretical critical collision frequency given by (16) is $\nu_c \approx 3.526$, and present results for varying ν from 1 to 3.5 and two values of ε: 1 and ε^{min}. We plot the electrostatic potential $\phi(x)$, resp. densities $n_i(x)$ and $n_e(x)$, in Figure 6, resp. in Figure 7.

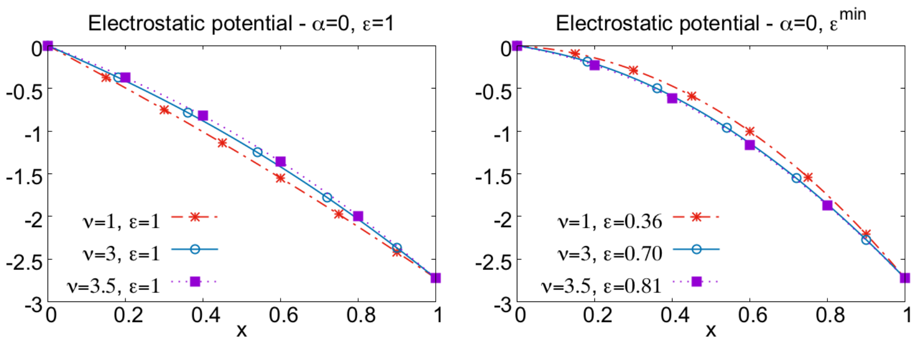

Figure 6: Electrostatic potential $\phi(x)$ for $\alpha = 0$, three values of ν: 1, 3 and 3.5. On the left: $\varepsilon = 1$, on the right: $\varepsilon = \varepsilon^{min}$.

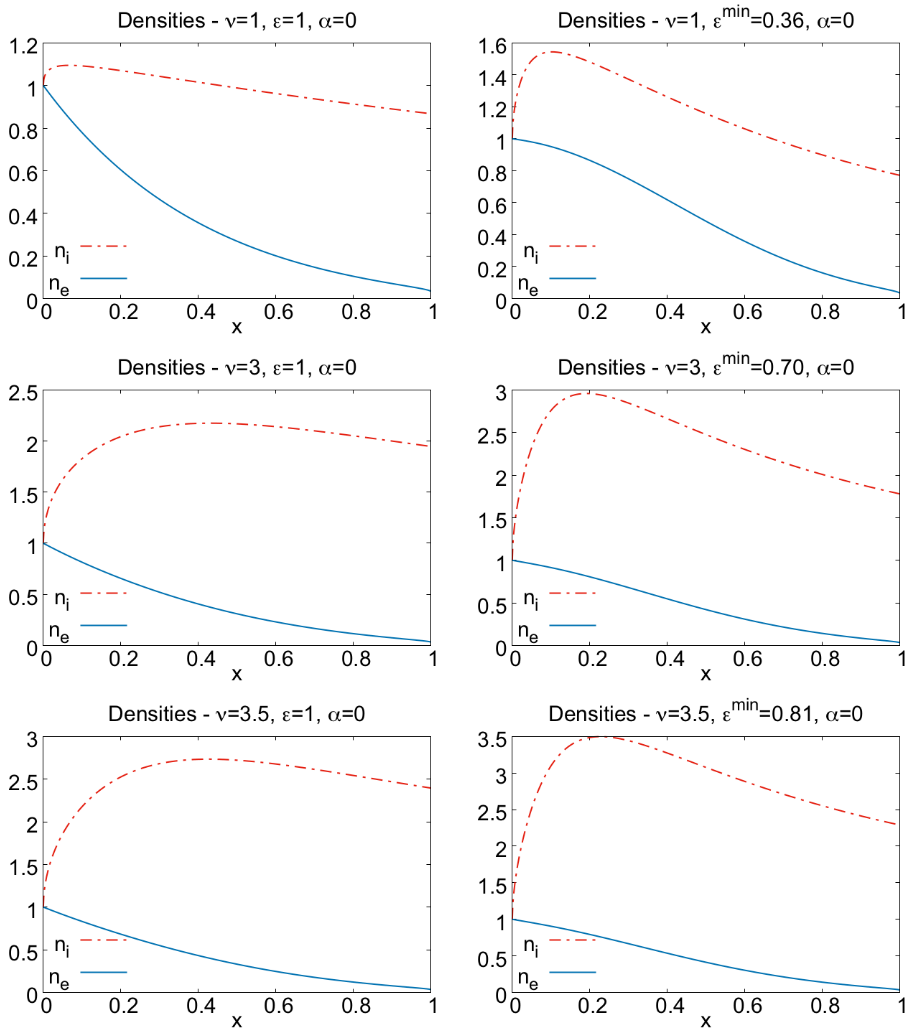

Figure 7: Ionic $n_i(x)$ and electronic $n_e(x)$ densities for $\alpha = 0$, three values of ν: 1, 3 and 3.5 (from top to bottom). On the left: $\varepsilon = 1$, on the right: $\varepsilon = \varepsilon^{min}$.

Then, ionic distribution function is presented in Figure 8 and the electronic one in Figure 9.

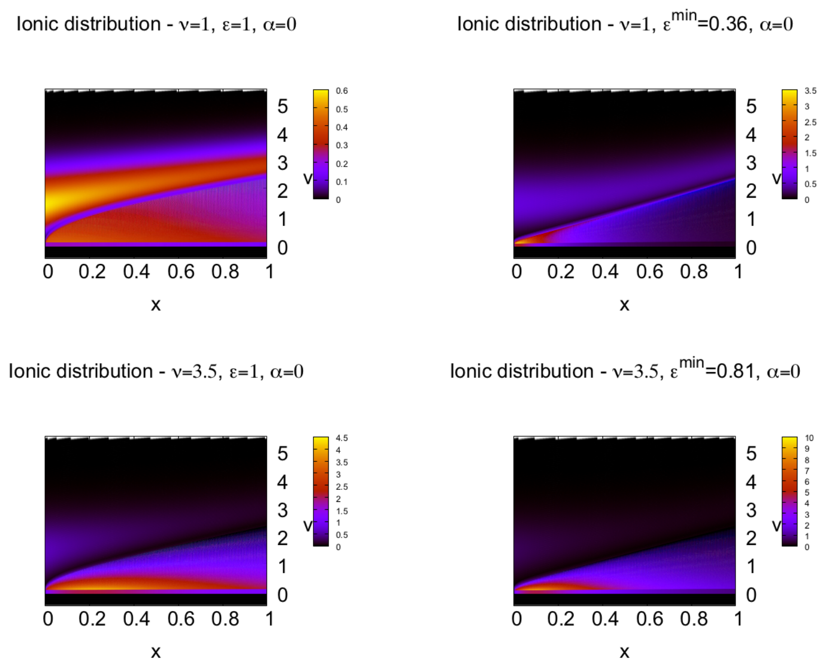

Figure 8: Ionic distribution function $f_i(x, v)$ for $\alpha = 0$, two values of ν: 1 and 3.5 (from top to bottom). On the left: $\varepsilon = 1$, on the right: $\varepsilon = \varepsilon^{min}$.

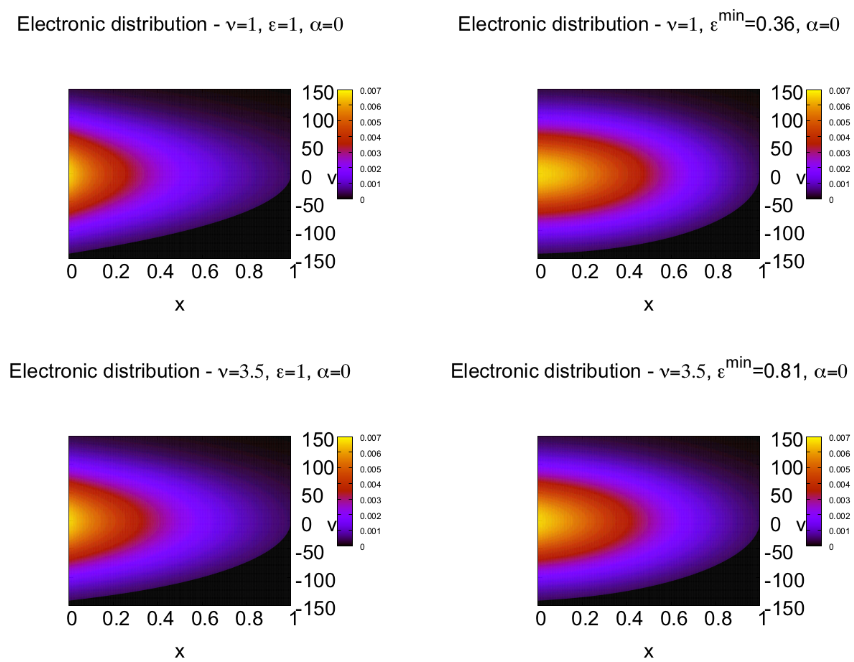

Figure 9: Electronic distribution function $f_e(x,v)$ for $\alpha = 0$, two values of ν: 1 and 3.5 (from top to bottom). On the left: $\varepsilon = 1$, on the right: $\varepsilon = \varepsilon^{min}$.

On the other hand, we fix $\nu = 0.2$ and present results for varying α from 0 to $0.9 < \alpha_c$ and two values of ε: 1 and ε^{min}. Figures 10, 11, 12 and 13 represent respectively the electrostatic potential, the densities, the ionic distribution function and the electronic one.

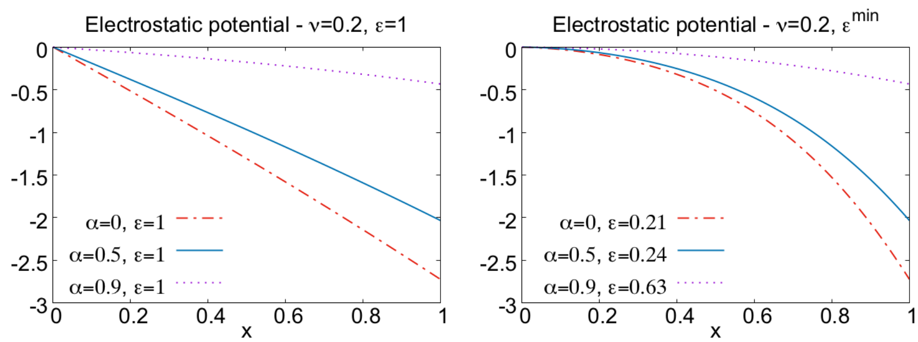

Figure 10: Electrostatic potential $\phi(x)$ for $\nu = 0.2$, three values of α: 0, 0.5 and 0.9. On the left: $\varepsilon = 1$, on the right: $\varepsilon = \varepsilon^{min}$.

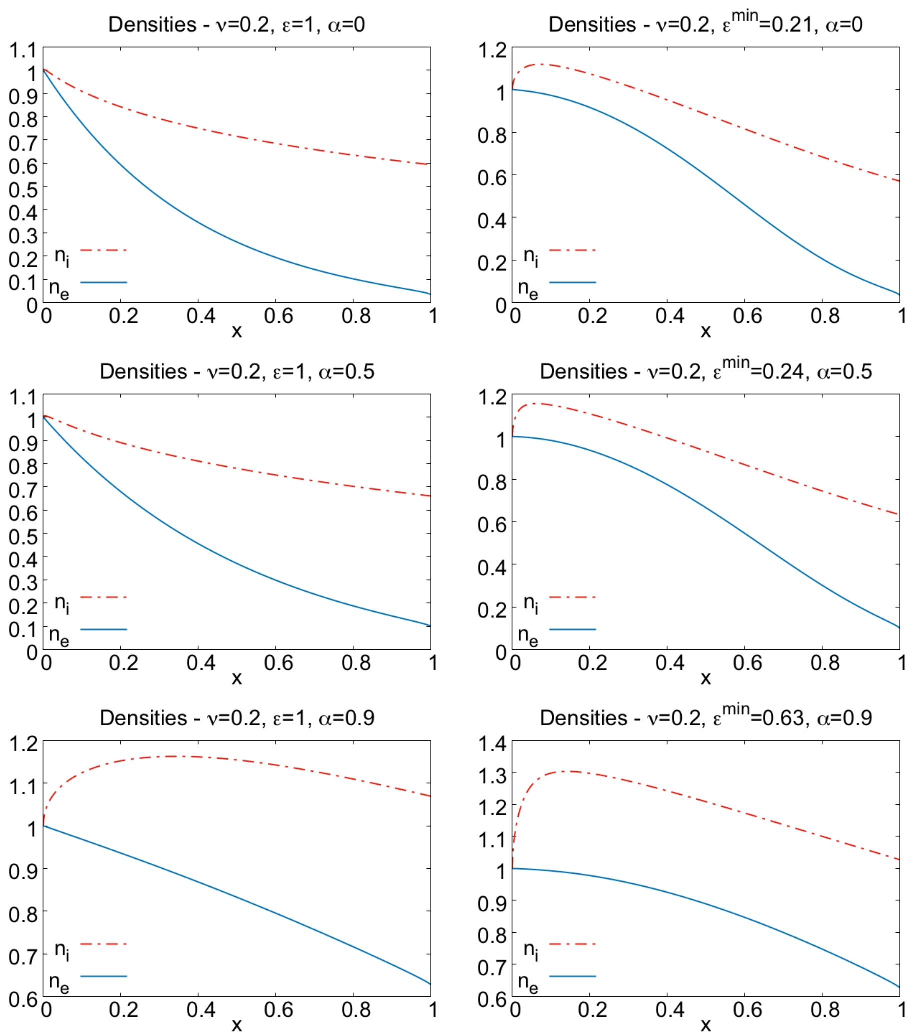

Figure 11: Ionic $n_i(x)$ and electronic $n_e(x)$ densities for $\nu = 0.2$, three values of α: 0, 0.5 and 0.9 (from top to bottom). On the left: $\varepsilon = 1$, on the right: $\varepsilon = \varepsilon^{min}$.

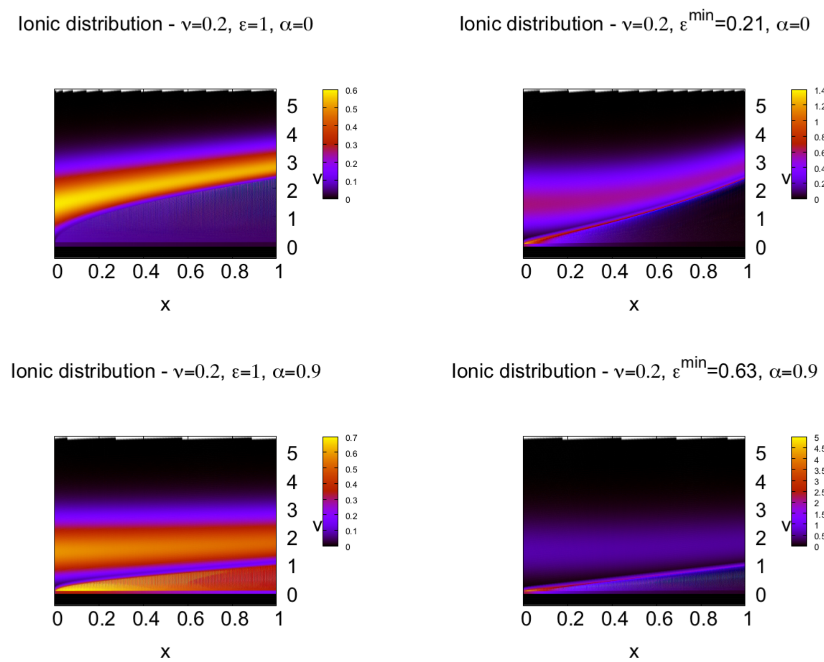

Figure 12: Ionic distribution function $f_i(x, v)$ for $\nu = 0.2$, two values of α: 0 and 0.9 (from top to bottom). On the left: $\varepsilon = 1$, on the right: $\varepsilon = \varepsilon^{min}$.

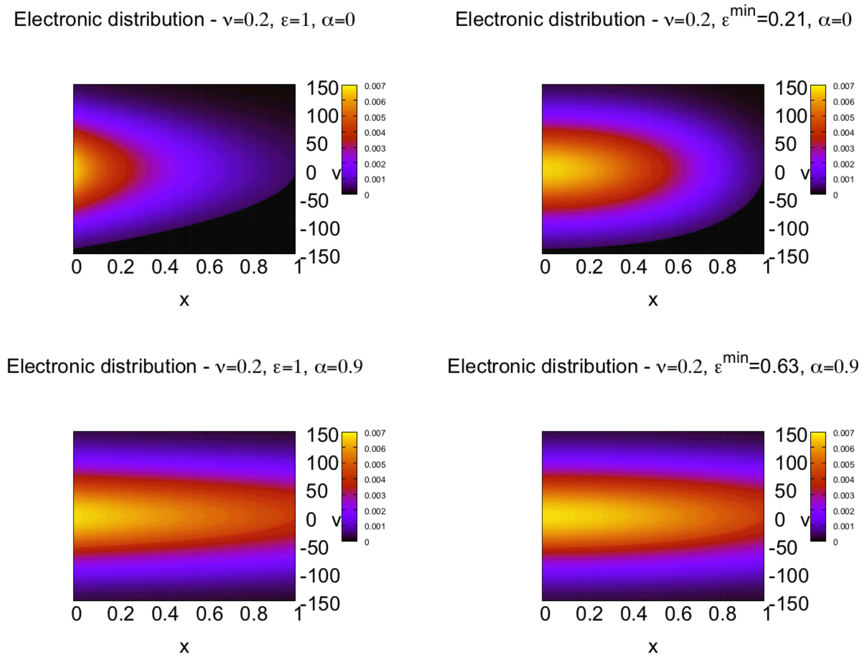

Figure 13: Electronic distribution function $f_e(x, v)$ for $\nu = 0.2$, two values of α: 0 and 0.9 (from top to bottom). On the left: $\varepsilon = 1$, on the right: $\varepsilon = \varepsilon^{min}$.

Interpretation. For the ions distribution function f_i, we observe on Figures 8 and 12 that increasing the collision frequency ν or diminishing the normalized Debye length ε results in in a stronger diffusion effect. Moreover, whatever the value of $\nu > 0$ is, f_i is non zero near the line $v = 0$ which is the expected effect of the collision operator (4). On Figure 8, we observe that for a near critical collision frequency $\nu \approx \nu_c$, there is some concentration of the ions distribution function in the vicinity of the line $v = 0$ while we can still observe low values of f_i for $v > \sqrt{-2\phi(x)}$. These results evidence the competition between the collision operator (4) which tends to relax the ions density f_i towards the mono kinetic density $n_i(x)\delta_{v=0}$ and the transport of the incoming boundary condition f_i^{inc} (78) from $x = 0$ to $x = 1$ with a damping effect. As for the electrons distribution function f_e, since it does not experience collisions, there is no change as compared to the non collisional case [4].

Increasing the re-emission coefficient α increases the values of the potential at the wall ($x = 1$) as it is observed on Figure 10. It results in a charge separation at $x = 1$ which is increasing with α as observed in Figure 11. As for the charge density $n_i - n_e$, we see on Figure 11 that it remains non negative and that it vanishes at $x = 0$ (as expected). We also see that increasing ν tends to increase the local charge n_i near $x = 0$. The macroscopic ions density n_i does not seem to be C^1 at $x = 0$. It is not suprising since it satisfies the weakly singular Volterra integral equation (23).

To conclude this study, we plot ε^{min} as a function of $\frac{\nu}{\nu_c} \in [0, 1[$ for the three values of α considered previously (note that $\nu_c \approx 3.526$ for $\alpha = 0$, $\nu_c \approx 2.644$ for $\alpha = 0.5$ and $\nu_c \approx 0.583$ for $\alpha = 0.9$). Results are presented in Figure 14.

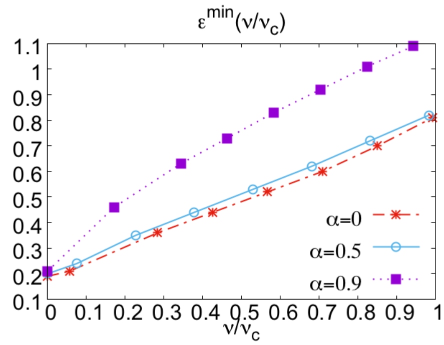

Figure 14: Minimal numerical value ε^{min} as a function of ν/ν_c for different values of α.

4.3. Collisional problems beyond the scope of Theorem 3.1

Finally, we are interested in simulations beyond the scope of Theorem 3.1. We notice that when taking $\nu > \nu_c$, the fixed point method hardly converges. In practice, we only have convergence for very large values of the normalized Debye length ε. The obtained densities are in this case a zoom on the space scale of the previous results. Specifically, we see the same behavior as in a window near $x = 0$ of Figures 7 or 11.

Our last numerical experiment, concerns an other physical scenario when considering an ionic incoming function f_i^{inc} for which the Bohm criterion (14) is not satisfied. We thus consider,

$$f_i^{\text{inc}}(v) = \frac{1}{\sqrt{2\pi}} e^{-\frac{v^2}{2}}, \ \forall v > 0.$$

This leads to $B_\alpha(f_i^{\text{inc}}) = -\infty$. We set the following physical parameters: $\alpha = 0$, $\nu = 0$ or 1, and $\varepsilon = 1$. We plot densities $n_i(x)$ and $n_e(x)$ in Figure

15. We can see that the inequality $n_i(x) - n_e(x) \geq 0$ (17) is not verified for x near zero. It seems to show that even in the collisional case the Bohm criterion (14) is a sharp condition to ensure the non negativity of the charge density.

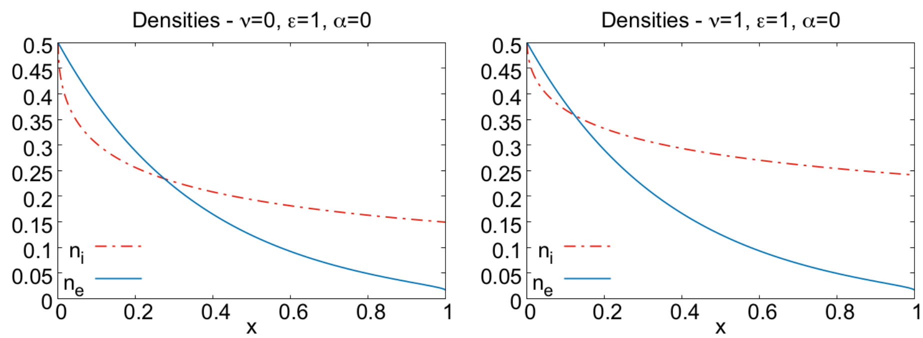

Figure 15: Ionic $n_i(x)$ and electronic $n_e(x)$ densities for $\alpha = 0$, two values of ν: 0 (on the left) and 1 (on the right).

5. Conclusion

In this work we proposed a numerical method to capture kinetic collisional sheaths. The method is based on the exact integrations of the transport equations by means of the characteristics curves and the numerical resolution of a non linear Poisson problem that has the form of an integro-differential equation. According to [4], this problem has a solution provided the inequalities (14),(17) and (18) are ensured. We thus designed a suitable discretization of the phase space together with adequate quadrature formulas that ensure easily the discrete analogue of these inequalities. We then presented some numerical experiments to assess mainly two physical scenarios. The first one was in the scope of our main result (Theorem 3.1) : when the Bohm criterion (14) holds and the different physical parameters are varied within appropriate bounds, we essentially observe that decreasing the Debye length or increasing the collision frequency results in a stronger diffusion effect on the ions distribution function. We also see some concentration of the distribution function near the line $v = 0$. There is a competition between the transport operator and the collision operator which yields in the extreme case some boundary layer near $x = 0$. Some parametric study between the Debye length and the collision frequency was carried out in order to assess a possible scaling between these two parameters. The second physical scenario mainly showed that when the Bohm criterion (14) is violated the charge density becomes negative near $x = 0$. It seems to show that the Bohm criterion (14) is a sharp condition to ensure the non negativity of the charge density. This work is up to our knowledge the very first one to propose a detailed numerical study of a fully kinetic collisional sheath model by means of a numerical method that strongly relies on a detailed analysis of the model under concern. It provided a range of physical parameters that is mathematically relevant. A possible perspective among others is to investigate asymptotic regimes $\varepsilon \to 0$ or $\nu \to +\infty$ though the model under concern may degenerate.

Acknowledgments

This work has been supported by the french "Agence Nationale pour la Recherche (ANR)" in the frame of the projects MUFFIN ANR-19-CE46-0004 and MoHyCon ANR-17-CE40-0027-01.

References

[1] Abdallah, N.B., Dolbeault, J., 2000. Relative entropies for kinetic equations in bounded domains. Arch. Rat. Mech. Anal. .

[2] Badsi, M., 2017. Linear electron stability for a bi-kinetic sheath model. Journal of Mathematical Analysis and Applications 453, 954–872.

[3] Badsi, M., 2020. Collisional sheath solutions of a bi-species vlasov-poisson-boltzmann boundary value problem. to appear in Kinetic and Related models, preprint on HAL: URL: https://hal.archives-ouvertes.fr/hal-02519292.

[4] Badsi, M., Campos Pinto, M., Després, B., 2016. A minimization formulation of a bi kinetic sheath. Kinetic and related models 9.

[5] Beale, J., Majda, A., 1982. Vortex methods. ii. high order accuracy in two and three dimensions,. Mathematics of computation 39.

[6] Bostan, M., Gamba, I., Goudon, T., Vasseur, A., 2010. Boundary value problems for the stationary vlasov-boltzmann-poisson equation. Indiana Univ. Math. 59.

[7] Campos-Pinto, M., Charles, F., 2016. Uniforme convergence of a linearly transformed particle method for the vlasov-poisson system. SIAM Journal of Numerical Analysis 54.

[8] Chen, F.F., 1984. Introduction to Plasma Physics and controlled fusion. Springer.

[9] Cohen, A., Perthame, B., 2000. Optimal approximations of transport equations by particle and pseudoparticle methods. SIAM J. Math.Anal. .

[10] Cottet, G.H., Raviart, P.A., 1984. Particle methods for the one-dimensional vlasov-poisson equations. SIAM Journal of Numerical Analysis , 52–76.

[11] Crouseilles, N., Respaud, T., Sonnendrucker, E., 2009. A forward semi-lagragian method for the numerical solution of the vlasov equation. Computer Physics Communications .

[12] Degond, P., F.Deluzet, 2017. Asymptotic-preserving methods and multiscale models for plasma physics. Journal of Computational Physics 336.

[13] Dubroca, B., R.Duclous, Filbet, F., 2012. Analysis of a high order finite volume scheme for the vlasov-poisson-system. Discrete Contin. Dyn. Syst 5, 283–305.

[14] Feldman, M., HA, S., Slemrod, M., 2005. A geometric level-set formulation of a plasma sheath interface. Arch. Rat. Mech. Anal. 178, 81–123.

[15] Gérard-Varet, D., Han-Kwan, D., Rousset, F., 2013. Quasineutral limit of the euler-poisson system for ions in a domain with boundaries. Indiana Univ. Math. J. 62 , 359–402.

[16] Heth, R., Gamba, I., Morrisson, P., Michler, C., 2012. A discontinuous galerkin method for the vlasov-poisson system. Journal of Computational Physics 231, 1140–1174.

[17] Jin, S., 1999. Efficient asymptotic-preserving (ap) schemes for some multiscale kinetic equations. SIAM J. Sci. Comput. 21.

[18] Laguna, A., Pichard, T., Magin, T., Chabert, P., Bourdon, A., Massot, M., 2019. An asymptotic preserving well-balanced scheme for the isothermal fluid equations in low-temperature plasma applications. Preprint HAL : https://hal.archives-ouvertes.fr/hal-02116610/document .

[19] Manfredi, G., Coulette, D., 2016. Kinetic simulations of the chodura debye sheath for magnetic fields with grazing incidence. arXiv:1509.04479v2 .

[20] Manfredi, G., Devaux, S., 2008. Plasma-wall transition in weakly collisional plasmas. AIP conference proceedings .

[21] M.Badsi, Merhemberger, M., Navoret, L., 2018. Numerical stability of plasma sheath. Esaim: proceedings 64, 17–36.

[22] Raviart, P.A., 1983. An analysis of particle methods. Numerical methods in fluid dynamics .

[23] Riemann, K., 1991. The bohm criterion and sheath formation. Physics of Plasmas .

[24] Riemann, K., 2003. Kinetic analysis of the collisional plasma-sheath transition. Journal of Physical D : Applied Physics 38.

[25] Sheridan, T., 2001. Solution of the plasma sheath equation with a cool maxwellian ion source. AIP Publishing .

[26] Sheridan, T., J.Gore, 1991. Collisional plasma sheath model. Phys. Fluids B .

[27] Stangeby, P., 2000. The Plasma Boundary of Magnetic Fusion Devices. Institute of Physics Publishing.

[28] Tonks, L., Langmuir, I., 1929. A general theory of the plasma of an arc. Physical review 34.

[29] Valsaque, F., Manfredi, G., 2001. Numerical study of plasma wall transition in an obligque magnetic field. Journal of nuclear materials .